Arabidopsis Small Rubber Particle Protein Homolog SRPs Play Dual Roles as Positive Factors for Tissue Growth and Development and in Drought Stress Responses[1][OPEN]

Eun Yu Kim, Ki Youl Park, Young Sam Seo[2], and Woo Taek Kim*

Department of Systems Biology, College of Life Science and Biotechnology, Yonsei University, Seoul 120-749, Korea

Lipid droplets (LDs) act as repositories for fatty acids and sterols, which are used for various cellular processes such as energy production and membrane and hormone synthesis. LD-associated proteins play important roles in seed development and germination, but their functions in postgermination growth are not well understood. Arabidopsis (*Arabidopsis thaliana*) contains three SRP homologs (SRP1, SRP2, and SRP3) that share sequence identities with small rubber particle proteins of the rubber tree (*Hevea brasiliensis*). In this report, the possible cellular roles of SRPs in postgermination growth and the drought tolerance response were investigated. Arabidopsis SRPs appeared to be LD-associated proteins and displayed polymerization properties in vivo and in vitro. *SRP*-overexpressing transgenic Arabidopsis plants (*35S:SRP1*, *35S:SRP2*, and *35S:SRP3*) exhibited higher vegetative and reproductive growth and markedly better tolerance to drought stress than wild-type Arabidopsis. In addition, constitutive over-expression of *SRPs* resulted in increased numbers of large LDs in postgermination seedlings. In contrast, single (*srp1*, *35S:SRP2-RNAi*, and *srp3*) and triple (*35S:SRP2-RNAi/srp1srp3*) loss-of-function mutant lines exhibited the opposite phenotypes. Our results suggest that Arabidopsis SRPs play dual roles as positive factors in postgermination growth and the drought stress tolerance response. The possible relationships between LD-associated proteins and the drought stress response are discussed.

Environmental stresses, including drought, high salinity, oxidative stress, and unfavorable temperatures, profoundly affect the growth and development of higher plants. Because of their sessile life cycle, plants have developed self-protective mechanisms to increase their tolerance to short- and long-term stresses by triggering diverse sets of signal transduction pathways and activating stress-responsive genes. The genetic and cellular mechanisms in response to abiotic stress have been widely documented in higher plants (Shinozaki and Yamaguchi-Shinozaki, 1996; Bray, 1997; Ishitani et al., 1997; Zhu, 2002; Bohnert et al., 2006; Shinozaki and Yamaguchi-Shinozaki, 2007; Vij and Tyagi, 2007).

Lipid droplets (LDs) are dynamic subcellular organelles enclosed by a monolayer of phospholipid. LDs act as repositories for fatty acids and sterols, which are used for energy production and membrane and hormone synthesis. LDs are also involved in various cellular processes, including intracellular protein storage, stress responses, and lipid signaling (Bartz et al., 2007; Zehmer et al., 2009; Carman, 2012; Herker and Ott, 2012; Murphy, 2012; Sun et al., 2013; Kory et al., 2015). LDs bud from the endoplasmic reticulum (ER), where they become enriched with triacylglycerols and subsequently enlarged, until they pinch off to form an LD (Chapman et al., 2012; Chapman and Ohlrogge, 2012; Jacquier et al., 2013). Several reports suggest that LD-associated proteins, such as fat-specific protein 27 (FSP27), SEIPIN, and PERILIPIN1 (Plin1), are key regulators of LD formation in mammals, *Drosophila*, and yeasts (Farese and Walther, 2009; Xu et al., 2012; Yang et al., 2012). After budding from the ER, LDs fuse with each other and expand. In adipocytes, Plin1 functions as an enhancer of FSP27-mediated lipid transfer and LD growth, indicating that Plin1 and FSP27 participate in LD formation and fusion (Sun et al., 2013). Enlarged LDs provide surfaces to allow the attachment of numerous LD-associated proteins, which are later displaced during shrinkage of LDs by lipolysis (Kory et al., 2015).

Because LDs are mainly present in seeds, studies on LD-associated proteins in higher plants have focused on seed development and germination (Chapman et al., 2013; Gidda et al., 2013; Horn et al., 2013; Szymanski et al., 2014). For example, oleosins regulate LD size in Arabidopsis (*Arabidopsis thaliana*) seed development

[1] This work was supported by grants from the Woo Jang Chun Special Project (PJ009106) funded by the Rural Development Administration, Republic of Korea, to W.T.K.

[2] Present address: The Korean Ginseng Research Institute, Korea Ginseng Corp., Daejeon 305-805, Korea.

* Address correspondence to wtkim@yonsei.ac.kr.

The author responsible for distribution of materials integral to the findings presented in this article in accordance with the policy described in the Instructions for Authors (www.plantphysiol.org) is: Woo Taek Kim (wtkim@yonsei.ac.kr).

E.Y.K., K.Y.P., and Y.S.S. performed the experiments; E.Y.K., K.Y.P., and W.T.K. analyzed the data; E.Y.K., K.Y.P., and W.T.K. planned the project and wrote the article; W.T.K. supervised the project and complemented the writing.

[OPEN] Articles can be viewed without a subscription.

www.plantphysiol.org/cgi/doi/10.1104/pp.16.00165

(Siloto et al., 2006). Arabidopsis SEIPINs modulate LD proliferation and neutral lipid accumulation in developing seeds (Cai et al., 2015). On the other hand, the cellular roles of LD-associated proteins in postgermination growth remain largely unraveled.

CaSRP1 (*Capsicum annuum* stress-related protein 1) was previously identified as a hot pepper small rubber particle protein (SRPPs) homolog (Hong and Kim, 2005). *CaSRP1* was induced in response to water stress in hot pepper plants. Constitutive over-expression of *CaSRP1* in transgenic Arabidopsis plants resulted in elevated growth and increased drought tolerance relative to wild-type Arabidopsis (Kim et al., 2010). CaSRP1 is evolutionarily related to SRPPs in rubber-producing plants (Wititsuwannakul et al., 2008). Rubber particles are single-membrane organelles that store rubber (cis-1,4-polyisoprene). Although rubber particles and LDs have different lipid compositions, their basic architectures are similar (Cornish et al., 1999). Thus, SRPP homologs may have common properties in the formation and biogenesis of rubber particles and/or LDs in rubber-producing and non-rubber-producing plants.

In this report, we identified and characterized three *SRPP* homologs, *SRP1*, *SRP2*, and *SRP3*, in Arabidopsis. The *SRP* genes were differentially expressed in various tissues and induced by abscisic acid (ABA) and a broad spectrum of abiotic stress, including drought, high salinity, and low temperature. *SRP*-overexpressing transgenic Arabidopsis plants (*35S:SRP1*, *35S:SRP2*, and *35S:SRP3*) exhibited higher vegetative and reproductive growth and markedly better tolerance to drought stress than wild-type Arabidopsis plants. In addition, ectopic expression of *SRPs* resulted in increased numbers of large LDs in postgermination seedlings. In contrast, single (*srp1*, *35S:SRP2-RNAi*, and *srp3*) and triple (*35S:SRP2-RNAi/srp1srp3*) loss-of-function mutant lines showed the opposite phenotypes. Arabidopsis SRPs appeared to be LD-associated proteins and displayed polymerization properties in vivo and in vitro. These results are discussed in light of the suggestion that Arabidopsis SRPs play dual roles as positive factors in postgermination growth and drought stress response. The possible relationships between LD-associated proteins and stress tolerance response are also discussed.

RESULTS

Arabidopsis Contains Three SRP Homologs

In our prior study, CaSRP1 was identified as a hot pepper small rubber particle protein homolog. *CaSRP1* was induced by dehydration in hot pepper plants, and *CaSRP1*-over-expressing transgenic Arabidopsis lines showed increased growth and enhanced drought tolerance relative to wild-type plants (Kim et al., 2010). In this study, we extended these findings to identify Arabidopsis SRP homologs. The Arabidopsis genome contains three SRP homologs: SRP1 (At1g67360), SRP2 (At2g47780), and SRP3 (At3g05500). Figure 1A represents the restriction map of the three *SRP* cDNAs. The predicted SRP1, SRP2, and SRP3 proteins are composed of 240 amino acids (M_r = 26.4 kD and pI value = 8.9), 235 amino acids (M_r = 26.6 kD and pI value = 4.4), and 246 amino acids (M_r = 27.2 kD and pI value = 8.3), respectively (Fig. 1A; Supplemental Fig. S1A).

The *35S:SRP-GFP* constructs were transiently expressed in tobacco (*Nicotiana benthamiana*) leaf cells by *Agrobacterium*-mediated transfection, after which protoplasts were prepared. Figure 1B shows that the fluorescent signals of all three SRP-GFP fusion proteins were mostly confined to the cytosolic fraction with spot- or dot-like structures. Subsequently, the *35S:Flag-SRP* fusion genes were transiently expressed in tobacco leaves, and the expressed proteins were characterized by immuno-blot analysis. The Flag-SRP proteins exhibited slightly different electrophoretic mobilities (33-35 kD and 35-37 kD), as detected by the anti-Flag antibody in tobacco total leaf extracts (Fig. 1C). These two shifted bands probably represented the truncated or modified forms of Flag-SRP fusion proteins due to unknown reasons. Flag-SRP1 and Flag-SRP2 proteins were exclusively found in the pellet fraction of the leaf extracts, while Flag-SRP3 was equally distributed in both the pellet and soluble fractions (Fig. 1C). When the Flag-SRP protein extracts were treated with 1% Triton X-100, most SRPs were detected in the soluble fractions, suggesting that SRPs are membrane associated.

SRPs share amino acid identities (34%-54%) with rubber tree (*Hevea brasiliensis*) SRPP (Supplemental Fig. S1, A and B). Rubber tree SRPP is a glycoprotein (Wititsuwannakul et al., 2008). To test whether Arabidopsis SRPs are glycosylated, a lectin-binding assay was performed using concanavalin A (Con A) column. As shown in Figure 1D, transiently expressed Flag-SRPs and endo-1,4-β-glucanase korrigan 1 (KOR1), a positive glycoprotein marker, bound to the Con A column. These lectin-binding activities were inhibited by methyl α-D-glucopyranoside, which has an affinity for Con A. Together, these results indicate that Arabidopsis SRPs contain lectin binding activities, suggesting that they are glycoproteins.

Arabidopsis *SRPs* Are Upregulated by ABA and Various Abiotic Stress Treatments

To analyze the spatial expression patterns of *SRPs* in various tissues of Arabidopsis, reverse transcription (RT)-PCR (Supplemental Fig. S2) and real-time quantitative (qRT)-PCR (Fig. 2A) were performed. The results showed that *SRP3* is a major transcript in all tissues examined, including seedlings, roots, leaves, stems, flowers, siliques, and developing seeds (Fig. 2A). *SRP1* and *SRP2* exhibited low levels of expression in Arabidopsis plants. One exception was that a high amount of *SRP2* transcript was detected in developing seeds (Fig. 2A). The histochemical *promoter-GUS* assay also revealed that *SRP3* is highly expressed throughout the Arabidopsis plants (Fig. 2B). Low levels of *SRP1* promoter activity were detected in the hydathodes,

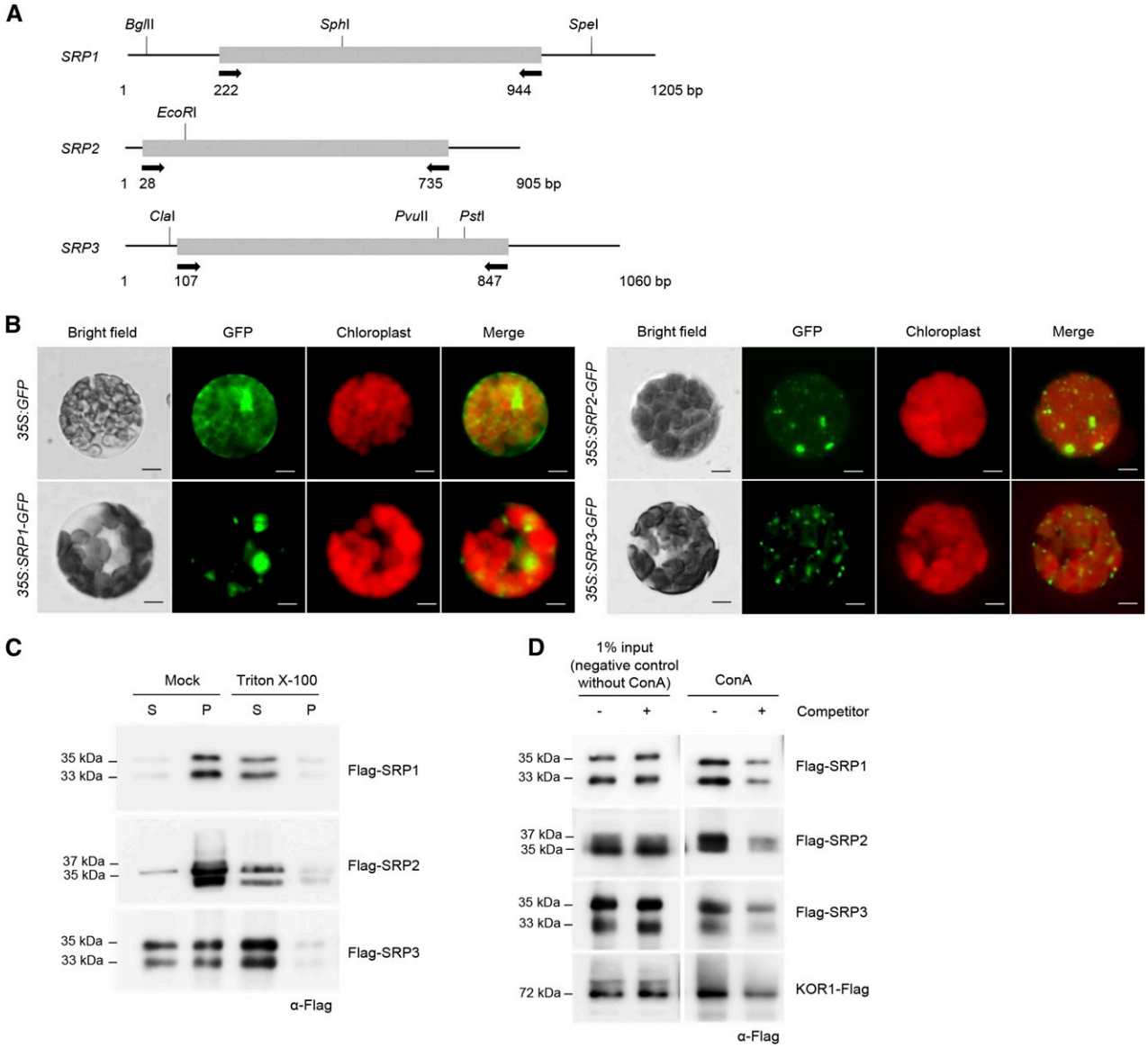

Figure 1. Characterization of Arabidopsis SRPs. A, Schematic structures of *SRPs*. Solid bars represent the coding regions. Solid lines depict the 5′-and 3′-untranslated regions. Arrows indicate the primers used for genotyping PCR and RT-PCR. Nucleotide sequences of the primers are listed in Supplemental Table S1. B, Subcellular localizations of SRPs in tobacco protoplasts. Protoplasts were obtained from tobacco leaves that transiently expressed *35S:SRP-GFP* fusion constructs. The GFP signals were detected by fluorescence microscopy under dark-field or light-field conditions. Scale bars = 10 μm. C, Membrane-association assay of SRPs. The *35S:Flag-SRP* fusion genes were transiently expressed in tobacco leaves. Soluble (S) and pellet (P) fractions of total leaf protein extracts were treated with Triton X-100 and subjected to immuno-blot analysis using anti-Flag antibody. D, Lectin-binding assay of SRPs. Total protein extracts were prepared from *Flag-SRP*-expressing tobacco leaves and were incubated with Con A-sepharose resin in the presence or absence of methyl α-D-glucopyranoside. Proteins eluted from the sepharose resin were analyzed by protein gel-blotting using anti-Flag antibody. Methyl α-D-glucopyranoside was used as a competitor to bind to Con A. KOR1 was used as a positive glycoprotein marker.

main veins of cotyledons, and newly dividing tissues, such as immature leaves, lateral root primordia, and root tips, whereas GUS activity of the *SRP2* promoter was barely detectable in the immature leaves of 7-d-old seedlings (Fig. 2B).

Further transcription analysis of *SRPs* was carried out using 7-d-old whole seedlings in response to ABA and various abiotic stress treatments. All three *SRP* transcripts were induced by 100 μM ABA treatment (0, 1.5, and 3 h; Fig. 2C). *SRP1* and *SRP3* were induced by different abiotic stresses, including drought (0, 1.5, and 3 h), low temperature (4°C for 0, 1.5, and 3 h), and high salinity (300 mM NaCl for 0 and 4.5 h), while expression of *SRP2* was enhanced selectively by dehydration (Fig. 2C).

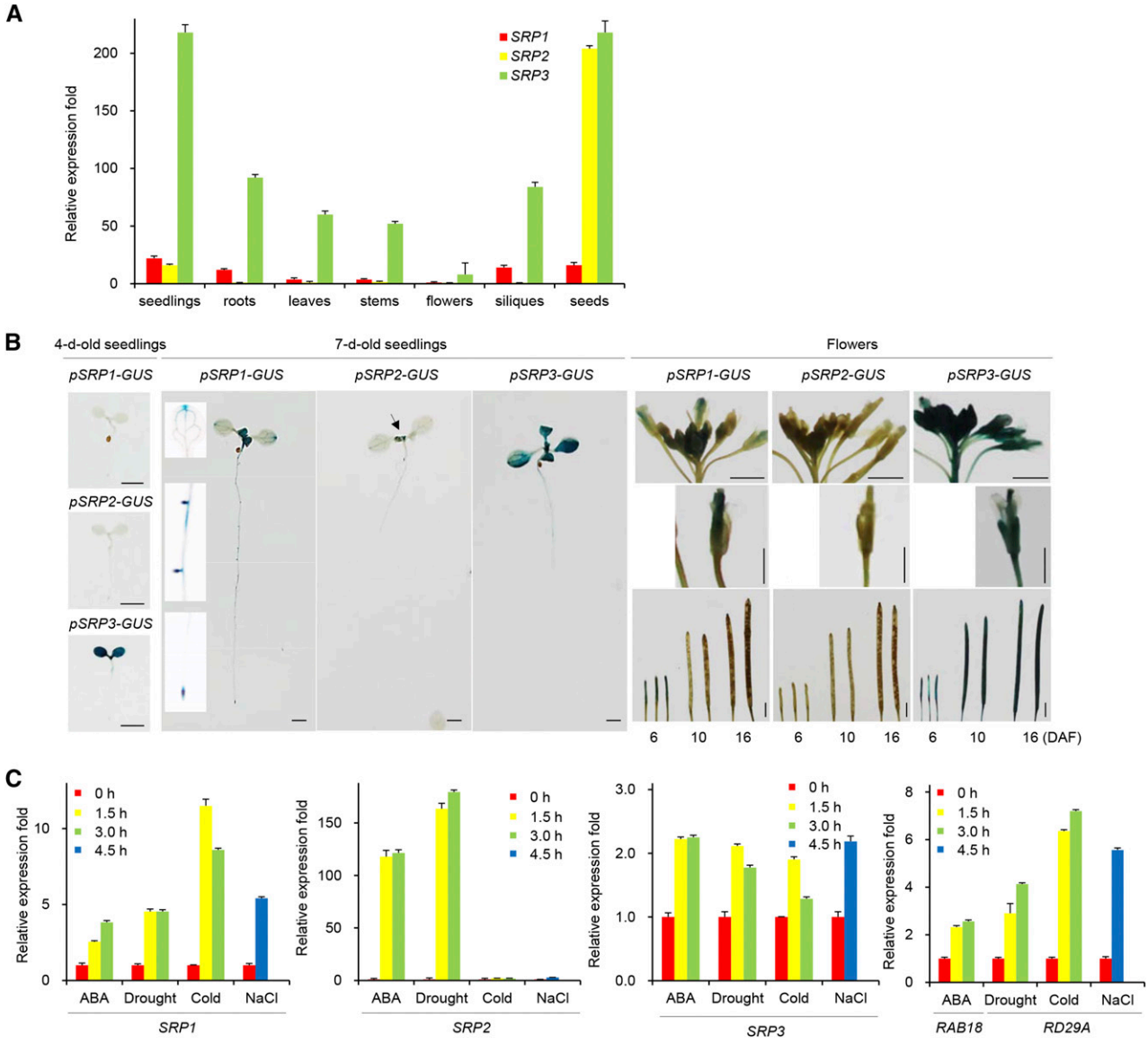

Figure 2. Expression of *SRPs*. A, Spatial expression patterns of *SRPs* in Arabidopsis. Transcript levels of *SRP1*, *SRP2*, and *SRP3* were analyzed in seedlings, roots, leaves, stems, flowers, siliques, and seeds by real-time qRT-PCR. The expression fold of *SRPs* was normalized to that of *glyceraldehyde-3-phosphate dehydrogenase C subunit*, which was used as a reference gene. Results are presented as means ± SD from three independent biological replicates. B, Promoter activities of *SRP1*, *SRP2*, and *SRP3* in developing Arabidopsis tissues. Histochemical GUS expression profiles in T3 *pSRP-GUS* transgenic plants were visualized by cyclohexylammonium salt staining for 16 h. Arrow indicates low level of *pSRP2-GUS* activity in the immature leaves of 7-d-old seedlings. DAF, day after flowering. Scale bars = 0.25 cm. C, qRT-PCR analysis of *SRPs*. Light-grown, 7-d-old, wild-type Arabidopsis seedlings were subjected to drought (0, 1.5, and 3 h), low temperature (4°C for 0, 1.5, and 3 h), high salinity (300 mM NaCl for 0 and 4.5 h), and 100 μM ABA (0, 1.5, and 3 h). Total RNA was extracted from the treated tissues and analyzed by qRT-PCR. *Glyceraldehyde-3-phosphate dehydrogenase C subunit* mRNA was used as an internal control for normalization. Error bars indicate means ± SD from three independent experiments.

Analysis (http://arabidopsis.med.ohio-state.edu) of upstream regions of three *SRP* genes indicated that they share similar cis-acting elements in their promoters, including *Dc3* Promoter-Binding Factor-1 (DPBF1) and -2 (DPBF2; Kim et al., 1997), MYB (Sablowski et al., 1994), related to ABI3/VP1-A (Kagaya et al., 1999), LEAFY consensus (Lamb et al., 2002), and ABA-responsive elements (ABRE)-like (Choi et al., 2000) binding sites (Supplemental Table S2). In addition, *SRP2* has additional regulatory elements in its promoter region, such as MYC2 (Abe et al., 1997), G-box binding factor 1/2/3 (de Vetten and Ferl, 1995), ABRE binding factors (Choi et al., 2000), auxin response factors (Ulmasov et al., 1999), and C-repeat/dehydration responsive element

binding factor 2 (Pla et al., 1993) binding motifs. These putative upstream cis-acting sequences in *SRPs* are in agreement with qRT-PCR and histochemical GUS data, suggesting that the expression of Arabidopsis *SRPs* is subject to control by developmental processes and abiotic stresses.

SRPs Play Positive Roles in Tissue Growth and Development

To investigate the cellular roles of SRPs, transgenic Arabidopsis plants (*35S:SRP1*, *35S:SRP2*, and *35S:SRP3*) that over-expressed full-length *SRPs* under the control of the 35S CaMV promoter were constructed (Supplemental Fig. S3A). In addition, T-DNA-inserted knock-out mutants of *SRP1* (*srp1*) and *SRP3* (*srp3*) were obtained (Supplemental Fig. S3, B and C). Because a loss-of-function mutant of *SRP2* was unavailable, RNAi-mediated knock-down transgenic lines of *SRP2* (*35S:SRP2-RNAi*) were generated (Supplemental Fig. S3D). The triple mutant line (*35S:SRP2-RNAi/srp1srp3*) was subsequently constructed by introducing the *35S:SRP2-RNAi* construct into the *srp1srp3* double knock-out mutant (Supplemental Figure S3E).

The phenotypic properties of the gain-of-function and loss-of-function progeny of *SRPs* were first investigated under normal growth conditions. As indicated in Figure 3A, the germination rates of the T4 over-expressing and mutant lines were indistinguishable at 1 to 5 d after imbibition, suggesting that SRPs may not be involved in the germination process under normal growth conditions. However, the postgermination growth rates of over-expressing and mutant lines were clearly different. We found that 4-d-old *SRP*-overexpressing seedlings displayed increased (1.4- to 1.7-fold) root growth; in contrast, the single (*srp1* and *srp3*) and triple (*35S:SRP2-RNAi/srp1srp3*) mutants exhibited shorter (0.5- to 0.7-fold) roots than the wild-type plants (Fig. 3B, left). The root growths of these plants were similar at 1 to 2 d after germination but became increasingly different at 3 to 8 d after germination (Fig. 3B, right). We noticed that the phenotypic difference of *35S:SRP2-RNAi* was not as clear as those of the *srp1* and *srp3* mutant lines. This was probably due to incomplete silencing of *SRP2* (Supplemental Fig. S3D). Alternatively, the expression level of *SRP2* is very low in most vegetative tissues (Fig. 2, A and B), and suppression of *SRP2*, in contrast to its over-expression, may not affect Arabidopsis growth under normal growth conditions.

Figure 3C shows that 2-week-old *35S:SRP* transgenic leaves were longer (1.3- to 1.4-fold) than the wild-type leaves, resulting in an approximately 1.5-fold increase in leaf surface area. The petiole length was also increased by 1.7 to 2.1 times in the *SRP*-over-expressing lines. In contrast, the loss-of-function *srp1*, *srp3*, and *35S:SRP2-RNAi/srp1srp3* mutant plants displayed, in general, the opposite phenotypes; they developed shorter leaves and petioles and consequently, their leaf area was reduced compared with wild-type plants (Fig. 3C). Again, the *35S:SRP2-RNAi* knock-down plants showed wild-type-like phenotypes. Overall, growth retardation was most severe in *srp3* and *35S:SRP2-RNAi/srp1srp3* (Fig. 3, B and C), suggesting that SRP3 is critical for leaf and root development.

The most striking phenotype of the *SRP* plants was that the *SRP* over-expressors grew more rapidly and bolted approximately 2 to 3 d earlier than the wild-type Arabidopsis plants did (Fig. 3D, top). Under our growth conditions, the majority of the wild-type plants bolted at 23 d after germination. However, the *35S:SRP* transgenic lines began bolting at 20 to 21 d after germination. At 25 d after germination, the inflorescence length of *SRP*-over-expressing plants was approximately 5 times longer than that of the control plants (Fig. 3D, bottom). By contrast, the single (*srp1* and *srp3*) and triple (*35S:SRP2-RNAi/srp1srp3*) mutant plants bolted 24 d after germination, indicating that suppression of *SRPs* resulted in delayed bolting phenotypes (Fig. 3D). Thus, these phenotypic analyses suggested that SRPs play positive roles in vegetative and reproductive growth in Arabidopsis.

The Tissue-Growth Phenotypes of the Over-expression and Loss-of-Function Mutants of *SRP*s Were Correlated with Cell Proliferation

To test whether the changes in root and leaf growth in the over-expression and loss-of-function mutants of *SRP*s were caused by alteration in cell division or elongation, the root tips and leaf cell layers were examined microscopically. The *SRP1*-, *SRP2*-, and *SRP3*-over-expressing plants exhibited an expanded proximal meristem (PM) zone in their root tips (Fig. 4A). Meristem cell number in the root tip PM zones of wild-type and over-expressing plants was 29.0 ± 0.5 and 35.0 ± 1.3, respectively, indicating that the three SRPs had similar positive impacts on root tip growth. In contrast, the *srp1*, *srp3*, and *35S:SRP2-RNAi/srp1srp3* mutant plants displayed a reduced number of meristem cells (22.0 ± 1.0, 19.0 ± 0.7, and 18.0 ± 0.3, respectively) in their root tip PM zones. *35S:SRP2-RNAi* knock-down root tips showed wild-type-like phenotypes. In addition, the *35S:SRP* transgenic leaves possessed smaller and more populated cells in both the epidermal and mesophyll layers relative to wild-type leaves (Fig. 4B). Figure 4B also shows that the *srp1*, *srp3*, and *35S:SRP2-RNAi/srp1srp3* mutant plants possessed lager and less dense cells in their leaves. These results indicate that the *SRP* over-expressors contained an increased number of cells in both the root and leaf tissues, while loss-of-function of *SRP1* and *SRP3* resulted in decreased cell number. Thus, it is likely that the enhanced growth that resulted from *SRP* over-expression was correlated with cell proliferation rather than cell elongation.

SRPs Participate in the Positive Regulation of Drought Stress Responses

On the basis of the stress-induced expression profiles of *SRPs* (Fig. 2C), we anticipated that SRPs participate in stress tolerance responses in Arabidopsis. In

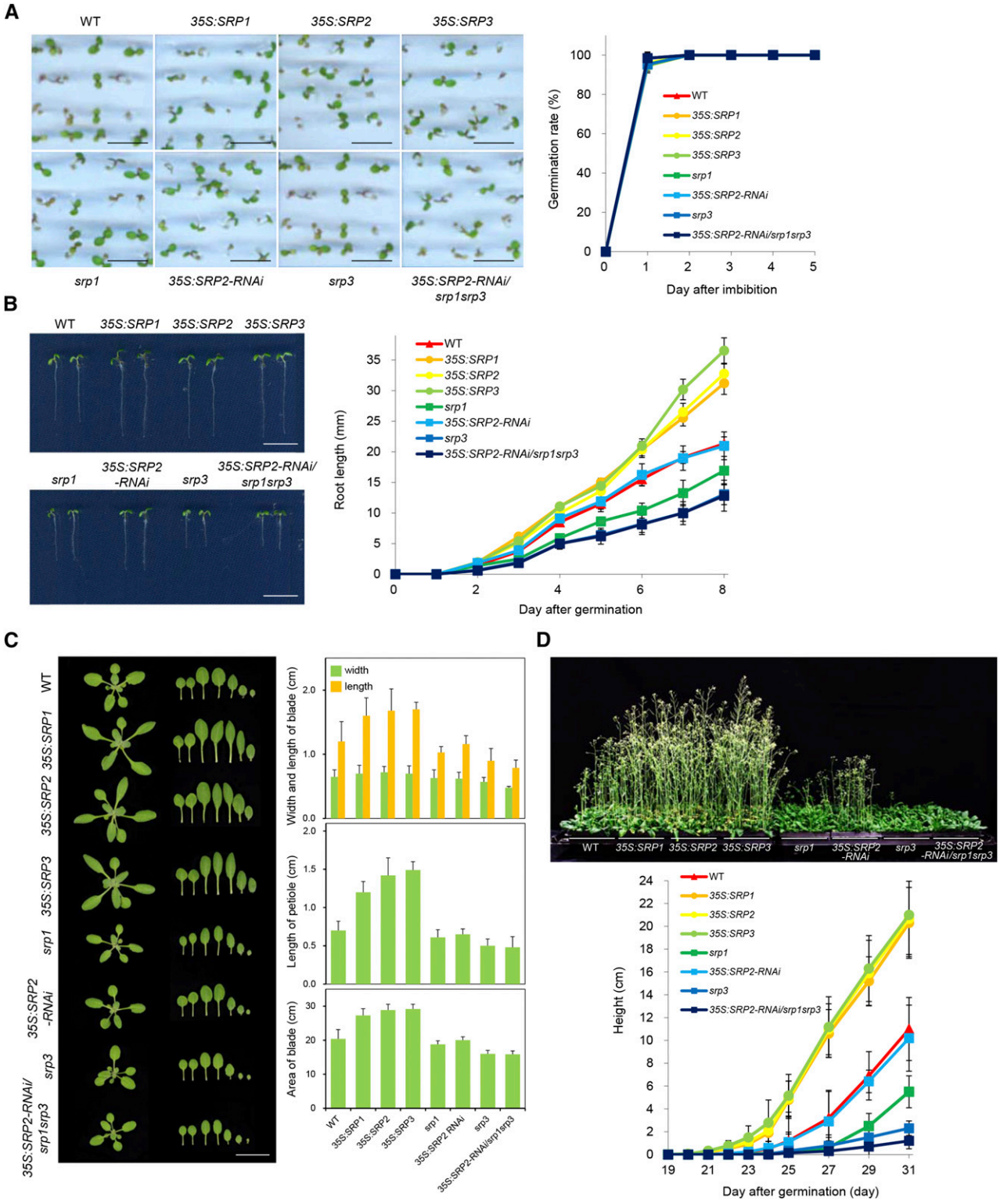

Figure 3. Phenotypic characterization of *SRP*-overexpressing and loss-of-function *srp* mutant plants. A, Germination assay. Left: wild-type (WT), *SRP*-over-expressing, and *srp* mutant seeds were germinated on half-strength Murashige and Skoog medium. Scale bars = 0.5 cm. Right: germination rates with respect to radicle emergency were determined 1 to 5 d after imbibition. Error bars indicate means ± SD (n = 80). B, Root growth. Left: morphological comparisons of wild-type, *SRP*-over-expressing, and *srp* mutant seedlings 4 d after germination. Scale bars = 2.0 cm. Right: growth profiles of wild-type, *SRP*-over-expressing, and *srp* mutant early roots 1 to 8 d after germination. Error bars indicate means ± SD (n = 40). C, Leaf growth. Left: morphological

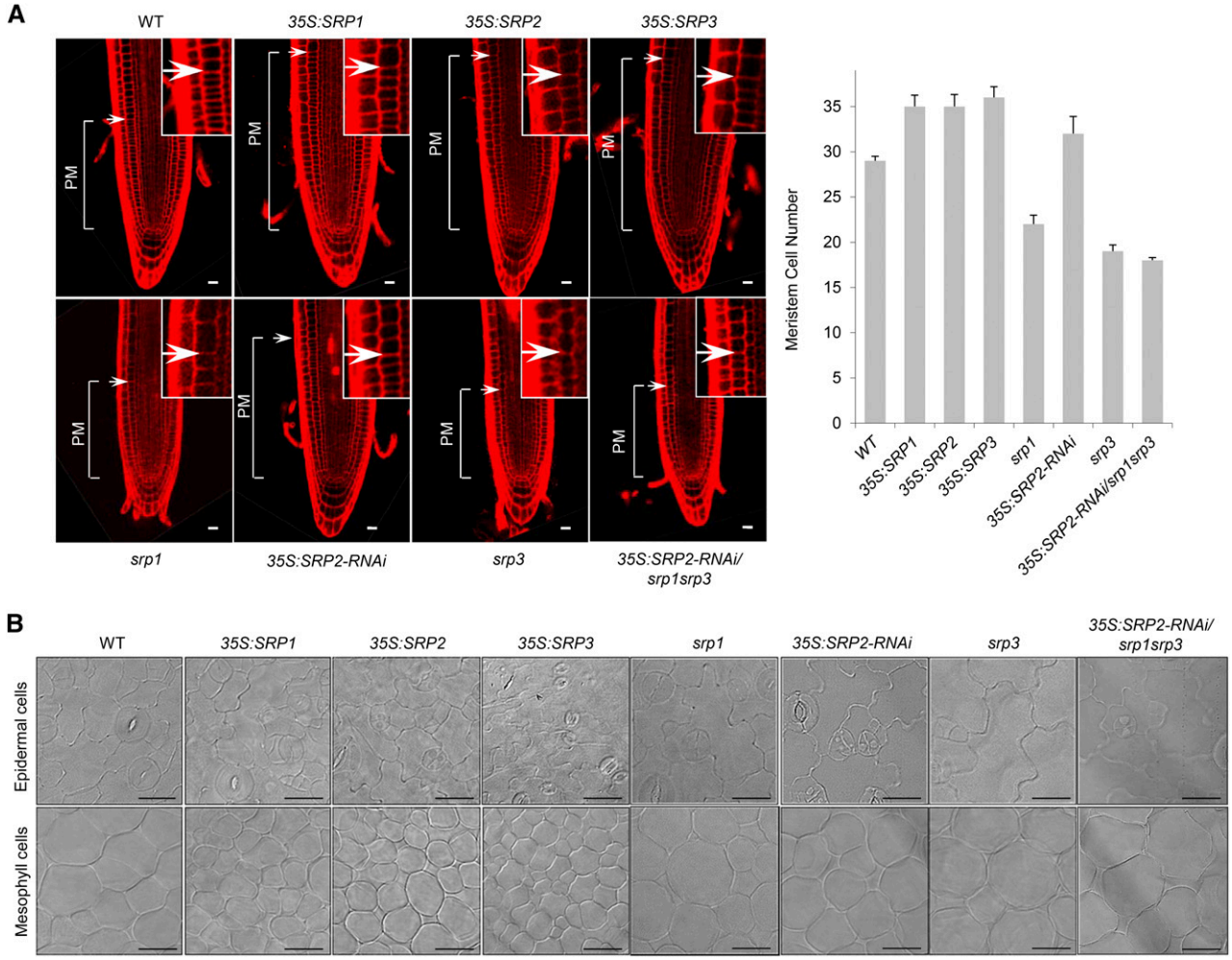

Figure 4. Cellular phenotypes of *35S:SRP* transgenic and *srp* mutant plants. A, Left: longitudinal sections of 3-d-old roots from wild-type, *SRP*-over-expressing, and *srp* mutant plants. Vertical lines indicate the PM. Arrows represent the transition zone between the PM and elongation-differentiation zones. The insets show a magnified transition zone. Root sections were stained with propidium iodide and visualized by confocal microscopy. Right: measurement of meristem cell number. Error bars indicate means ± SD (n = 30). B, Different cell sizes in wild-type, *SRP*-over-expressing, and *srp* mutant leaves. The epidermal and mesophyll cell layers of 5-d-old leaves were treated with chloral hydrate, a tissue-clearing reagent. The image was visualized by light microscopy. Scale bars = 20 μm.

particular, all three *SRPs* are upregulated in response to dehydration (Fig. 2C). Therefore, the survival ratios of *SRP*-over-expressing and mutant plants were monitored after drought treatment. Light-grown, 2-week-old wild-type and *SRP* over-expressors were subjected to dehydration by withholding water for 10 d, which resulted in complete drying of the potted soil. These water-stressed plants were irrigated, and their survival rates were analyzed 3 d after reirrigation. The results indicated that the *SRP* over-expressors were more tolerant to water stress than the wild-type plants. The survival ratios of *35S:SRP1*, *35S:SRP2*, and *35S:SRP3* were 65% (59 of 91), 66% (59 of 89), and 58% (47 of 81), respectively, which are 2.2- to 2.5-fold higher than that (27%, 24 of 89) of the wild-type plants (Fig. 5A, left). In contrast, the loss-of-function progeny were highly sensitive to mild dehydration treatment. Three-week-old wild-type and mutant plants were exposed to water

Figure 3. (*Continued.*)
comparisons of 2-week-old rosettes from wild-type, *SRP*-over-expressing, and *srp* mutant plants. Scale bars = 2.0 cm. Right: quantification of the dimensional parameters of the second leaf. Detached second leaves were analyzed using the SCIONIMAGE program. Error bars indicate means ± SD (n = 40). D, Bolting. Top: bolting phenotypes of wild-type, *SRP*-over-expressing, and *srp* mutant plants. Bottom: growth rates of the inflorescence stems of wild-type, *SRP*-overexpressing, and *srp* mutant plants were monitored 19 to 31 d after germination. Error bars indicate means ± SD (n = 80).

stress for 8 d, and the recovery rates were measured after 3 d of rewatering. After this mild drought treatment, 100% (96 of 96) of wild-type plants resumed growth, while the survival rates of the *srp1*, *35S:SRP2-RNAi*, *srp3*, and *35S:SRP2-RNAi/srp1srp3* plants were 40% (35 of 88), 7% (6 of 92), 24% (23 of 94), and 0% (0 of 91), respectively (Fig. 5A, right). Triple *35S:SRP2-RNAi/srp1srp3* mutant plants were extremely sensitive to dehydration, suggesting that the three SRP homologs play interconnected roles to cope with conditions of water

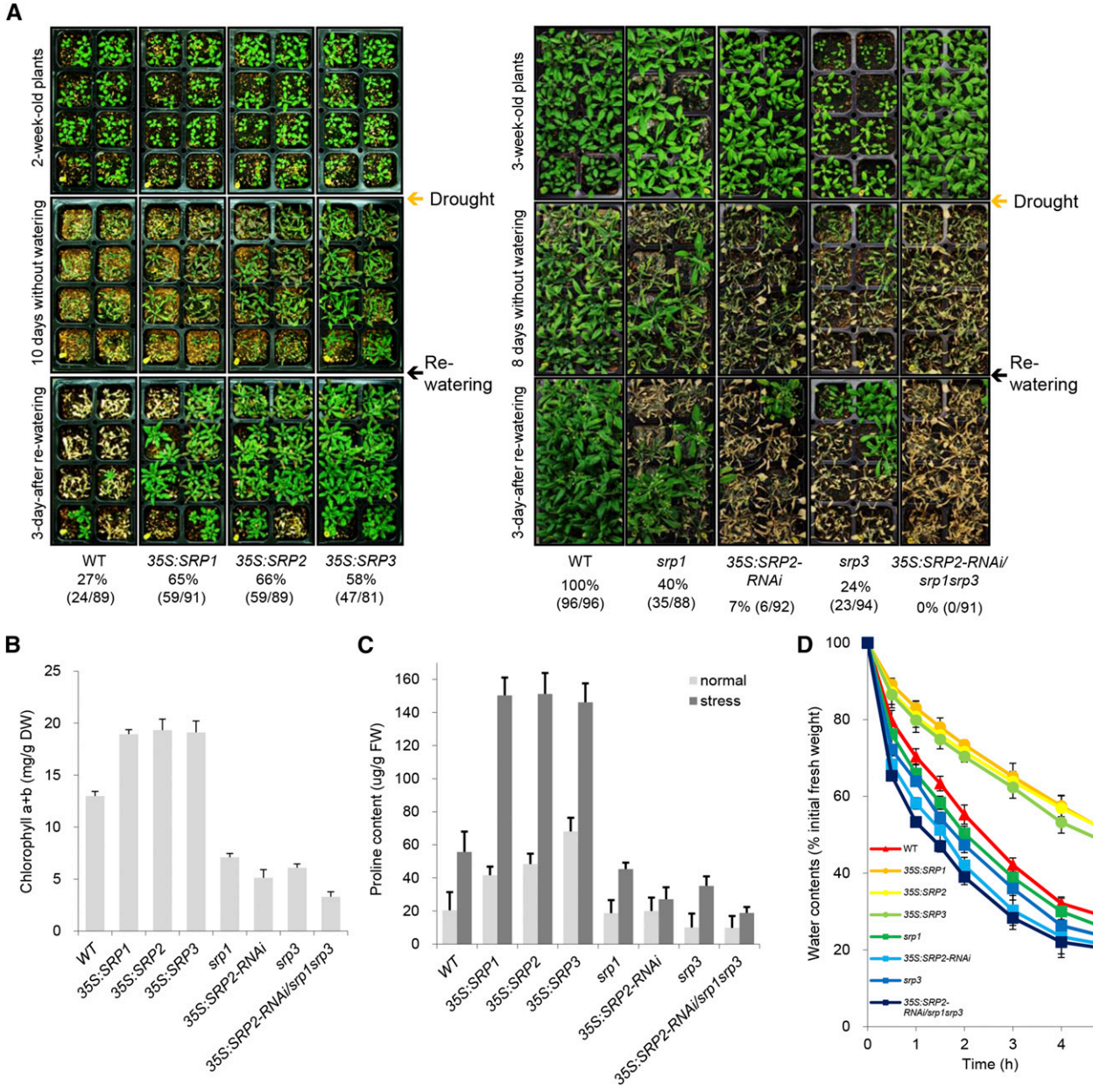

Figure 5. Drought sensitivity of wild-type, *SRP*-over-expressing, and *srp* mutant plants. A, Left: Light-grown, 2-week-old wild-type (WT) and *SRP* over-expressors (*35S:SRP1*, *35S:SRP2*, and *35S:SRP3*) were further grown for 10 d without irrigation. Plants were rewatered, and the survival rates were determined 3 d after rewatering. Right: wild-type and *srp* mutant (*srp1*, *35S:SRP2-RNAi*, *srp3*, and *35S:SRP2-RNAi/srp1srp3*) plants were grown for 3 weeks under normal growth conditions. After 8 d of desiccation, the plants were recovered by rewatering, and the number of surviving plants was counted 3 d after irrigation. B, Total chlorophyll amounts (mg/g DW) in wild-type, *SRP*-over-expressing, and *srp* mutant leaves after drought stress. Error bars indicate means ± SD ($n = 20$). C, Pro content of wild-type, *SRP*-over-expressing, and *srp* mutant leaves before (gray bars) and after (dark bars) water stress. Error bars indicate means ± SD ($n = 15$). D, Measurement of the rate of water loss in cut rosettes from wild-type, *SRP*-over-expressing, and *srp* mutant plants. Detached rosette leaves were subjected to desiccation for 0 to 5 h at room temperature. Water loss is represented as the percentage of the initial fresh weight of the detached rosette leaves. Error bars indicate means ± SD ($n = 8$).

deficit. It should be noted that the *35S:SRP2-RNAi* knock-down plants were markedly more susceptible to water stress than the *srp1* and *srp3* lines, suggesting a critical role for SRP2 in drought stress response. This view is consistent with the result that *SRP2* is specifically induced by dehydration stress (Fig. 2C).

In agreement with the survival rates, *SRP*-over-expressing leaves contained higher amounts of chlorophyll a + chlorophyll b (18.9 ± 0.5 mg/g dry weight [DW] to 19.3 ± 1.1 mg/g DW) than the wild-type leaves (12.9 ± 0.5 mg/g DW) after drought stress (Fig. 5B). As expected, the chlorophyll levels were decreased in the mutant leaves, with that of the triple *35S:SRP2-RNAi/srp1srp3* mutant leaves being most severely reduced (3.3 ± 0.5 mg/g DW). In addition, the Pro content of the *35S:SRP* leaves was up to 3.3 times higher than that of the wild-type leaves before and after drought treatment, while the Pro content of the mutant leaves was lower (Fig. 5C). These results indicate that the expression levels of *SRPs* are positively correlated with photosynthetic activity and the accumulation of osmoprotectants.

Finally, the cut rosette water loss assay indicated that *SRP*-over-expressing plants retained their leaf water more efficiently than the wild-type plants. When 3-week-old detached rosette leaves from wild-type and over-expressing plants were incubated at room temperature for 5 h under dim light, the wild-type leaves lost approximately 72% of their fresh weight relative to the starting weight, whereas the *SRP*-over-expressing leaves lost only 49% to 52% of their fresh weight (Fig. 5D). The loss-of-function mutant leaves displayed the opposite phenotypes. After 5 h of incubation, detached mutant leaves lost up to 71% to 80% of their fresh weights, indicating that more rapid water loss occurred in the mutant leaves than in the wild-type leaves (Fig. 5D). Collectively, the phenotypic analyses presented in Figure 5 strongly support the notion that the three SRP homologs play combinatory roles in the positive regulation of dehydration stress responses in Arabidopsis.

SRPs Are Related with Cell Wall Organization

The aforementioned results indicate that Arabidopsis SRPs are involved in tissue growth and development (Figs. 3 and 4) and in the tolerance to drought stress (Fig. 5), which indicates dual roles for SRPs in growth and stress responses. Therefore, more detailed phenotypic properties of *SRP* over-expressors and mutants were investigated. Because *SRP*-over-expressing tissues displayed an elevated cell proliferation rate and more rapidly growing phenotypes, and vice versa for mutant tissues (Figs. 3 and 4), we considered the possibility that the cell wall structures of these plants are affected by the expression levels of *SRPs*. Seed coat is often used to analyze cell wall structure (Stork et al., 2010). Thus, the seed coat structures of over-expressors and mutants of *SRPs* were examined by SEM. In general, the columella, which is the epidermal layer of the Arabidopsis seed coat, exhibited a hexagonal and volcano-shaped structure (Fig. 6A). Regular but enlarged columellae were observed in *SRP*-over-expressing seeds, resulting in less dense cell wall structures relative to the wild-type seeds (Supplemental Fig. S4). The columella of the *35S:SRP2-RNAi* knock-down plants showed wild-type-like structures. However, the typical hexagonal and volcano structures of the columellae were attenuated in the other loss-of-function mutants (*srp1*, *srp3*, and *35S:SRP2-RNAi/srp1srp3*). Furthermore, their epidermal cells displayed aberrant and irregular shapes, although their sizes were somewhat similar to those of wild-type seeds (Fig. 6A; Supplemental Fig. S4). *Wall-associated kinase 1* (*WAK1*), *FEI2*, and *pectin methylesterase* (*PME3*) are cell wall marker genes (Micheli, 2001; Xu et al., 2008; Steinwand and Kieber, 2010). WAK1 and FEI2 are receptor-like kinases that are required for cell wall expansion and synthesis of cell wall components, respectively. PME3 catalyzes the demethylesterification of pectin, which contributes to cell wall growth (Micheli, 2001). As shown in Figure 6B, all three cell wall marker genes were upregulated in the *SRP* over-expressors (1.4- to 14.8-fold), and in contrast, they were downregulated in the triple mutant plant (0.7-fold), relative to the expression levels in the wild-type plant (Fig. 6B). Overall, these results support the view that SRPs are involved in cell wall organization in Arabidopsis.

SRPs Are Colocalized to LDs in Tobacco Leaves

Horn et al. (2013) reported that LDAP1 and LDAP2 are LD-associated proteins in avocado (*Persea Americana*). Avocado LDAP1 and LDAP2 are homologs of SRP3. Like LDAP1 and LDAP2, SRP3 is localized at the surface of LDs in tobacco cells (Horn et al., 2013). The subcellular localization patterns of SRP1 and SRP2 were very similar to that of SRP3, suggesting that they are localized to LDs (Fig. 1B). To confirm these results, colocalization of SRPs and LDs were examined. As shown in Figure 7A, mature tobacco leaves contained few LDs detected by Nile red staining. LEAFY COTYLEDON 2 (LEC2) is a transcription regulator that increases number of LDs by promoting the expression of seed-specific genes and lipid accumulation (Cai et al., 2015). Consistent with previous results, *35S:LEC2*-infiltrated tobacco leaves exhibited increased number of LDs (Fig. 7B). When *35S:LEC2* and *35S:SRPs-GFP* constructs were coinfiltrated, the Nile red-stained LDs and SRPs-GFP fluorescent signals were well merged in tobacco leaves (Fig. 7C). Thus, it seems highly likely that SRPs and LDs are closely associated, suggesting that SRPs are localized to LDs.

SRPs Play Positive Roles in the Biogenesis of LDs

Subcellular colocalization studies suggest that SRP1, SRP2, and SRP3 are localized to LDs (Fig. 7). In both plant and mammalian systems, the development of LDs is closely linked to the optimal functioning of

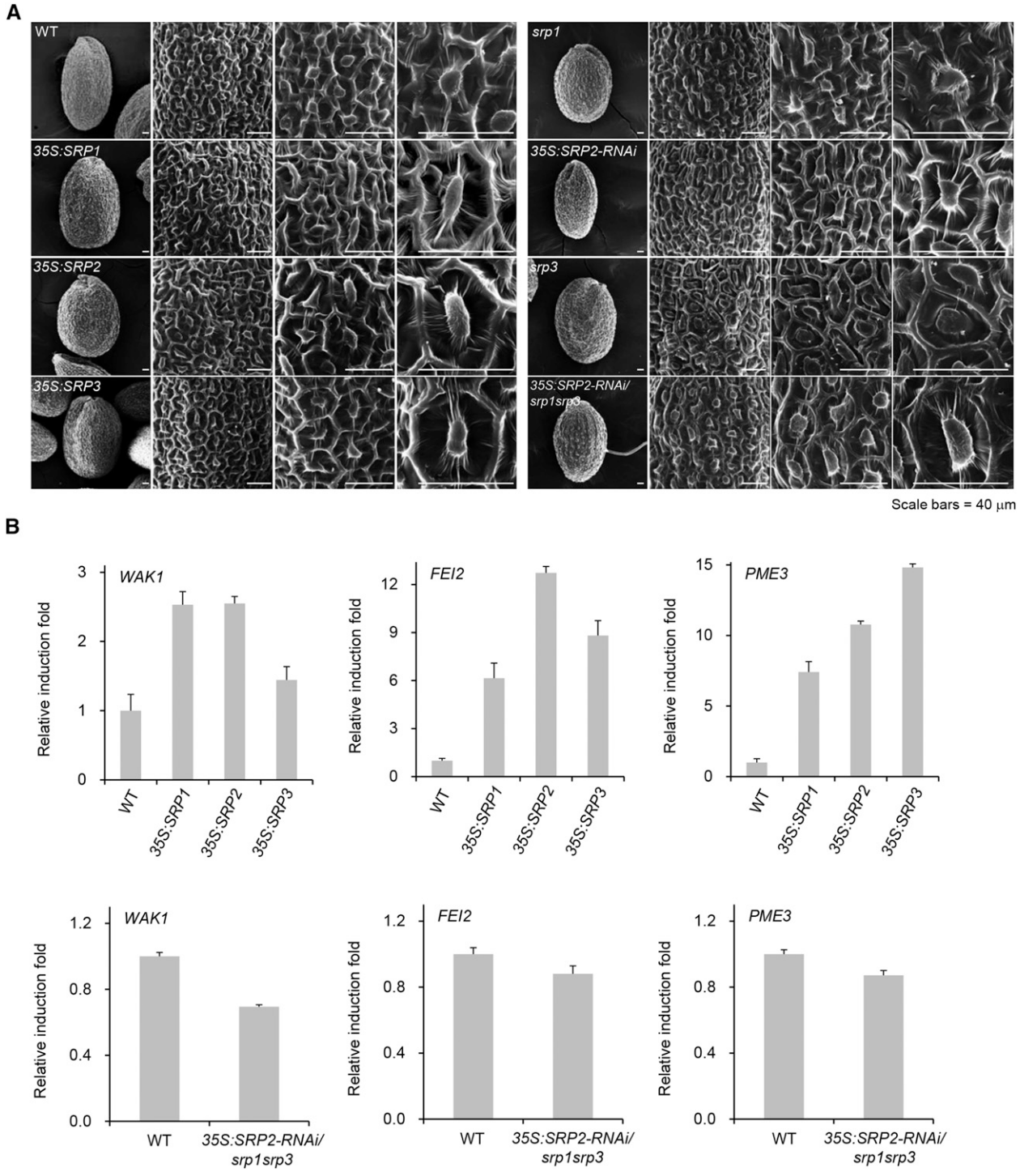

Figure 6. Surface structure of seed coats and the expression levels of cell wall-related genes. A, SEM analysis of dry seeds of wild-type (WT), *35S:SRP* transgenic, and *srp* mutant plants. Scale bar = 40 μm. B, Transcriptional changes in cell wall-modifying genes (*WAK1*, *FEI1*, and *PME3*) in *SRP*-over-expressing and mutant progeny relative to wild-type plants. Data represent means ± SD from three independent experiments.

LD-associated proteins (Guo et al., 2009; Wilfling et al., 2014). Therefore, we hypothesized that Arabidopsis SRPs are also involved in LD development. LDs are abundant in the dry-seed stage, and their numbers gradually reduce during germination and seedling establishment in Arabidopsis (Eastmond, 2006; Kim et al., 2011). We analyzed the size and number of cellular LDs in the 6-d-old seedlings of the *SRP* over-expressors and

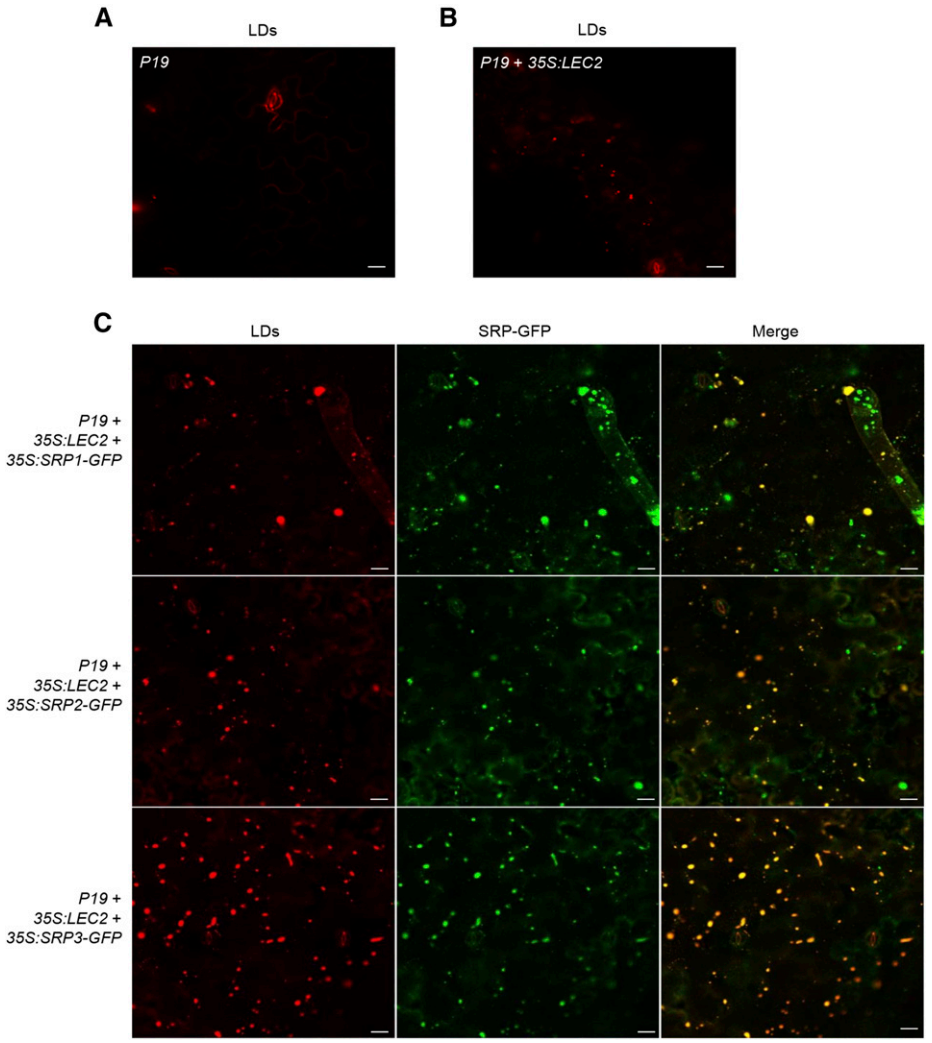

Figure 7. Colocalization of Arabidopsis SRPs to LDs. The *35S:P19* (A), *35S:P19* + *35S:LEC2* (B), and *35S:P19* + *35S:LEC2* + *35S:SRPs-GFP* (C) constructs were transiently expressed in tobacco leaves via *Agrobacterium*-mediated infiltration. P19, a viral suppressor of posttranscriptional gene-silencing, was used to increase infiltration efficiency. LEC2 was used to promote lipid accumulation and increase number of LDs. After 3 d of infiltration, leaves were stained using Nile red (2 μg/mL) and fluorescent signals were visualized via confocal microscopy. Red and green signals represented LDs and SRP-GFPs, respectively. Scale bars = 20 μm.

35S:SRP2-RNAi/srp1srp3 triple mutant plants by transmission electron microscopy (TEM). Various sizes of LDs were observed in the wild-type seedlings: approximately 9.8% of LDs were >2.5 μm in diameter, 19.7% were 2.0 to 2.5 μm, 16.4% were 1.5 to 2.0 μm, 32.8% were 1.0 to 1.5 μm, 16.4% were 0.5 to 1.0 μm, and 5.2% were 0.0 to 0.5 μm (Fig. 8A). However, in the *SRP*-over-expressing seedlings, numerous enlarged LDs were routinely detected. For example, 13.1% to 17.2% of the LDs were larger than 2.5 μm in diameter, and 22.1% to 34.7% were 2.0 to 2.5 μm (Fig. 8A). In contrast, only 0.1% to 1.3% of the LDs were 0.0 to 0.5 μm in diameter, which suggests that *SRP* over-expression resulted in an increased number of large LDs in the early seedlings. The opposite phenotypes were observed in the *35S:SRP2-RNAi/srp1srp3* mutant seedlings. As indicated in Figure 8A, the number of small-sized LDs (0.0-0.5 μm in diameter) was increased by up to approximately 15.0% in these plants. In addition, LDs with diameters >2.5 μm were rarely detected in the triple mutant seedlings. Thus, it is likely that SRPs are positively involved in the biogenesis of LDs. Alternatively, SRPs may inhibit the lipolysis of LDs by blocking LD-lipase interaction, thereby influencing LD morphology. Fatty acids, which are formed by the lipolysis of LD, are transported into the mitochondria and used to generate ATP via β-oxidation (Aon et al., 2014). qRT-PCR analysis revealed that the mRNA levels of both *cytochrome c oxidase 1* (*COX1*) and *COX2*, which encode the rate-limiting enzymes of the mitochondrial respiratory chain (Khalimonchuk and Rödel, 2005; Fontanesi et al., 2008), were correlated with *SRP* mRNA levels. *COX1* and *COX2* were up-regulated and down-regulated in the *SRP* over-expressors and *35S:SRP2-RNAi/srp1srp3* mutant seedlings, respectively (Fig. 8B). These data indicate that the biogenesis, rather than the lipolysis, of LDs was affected by the expression of *SRPs*. Collectively, these results suggest that SRPs play positive roles in determining the number and size of LDs.

SRPs Exhibit Polymerization Properties in Vivo and in Vitro

Rubber tree SRPP exhibits latex coagglutination activity (Wititsuwannakul et al., 2008). In addition, bacterially

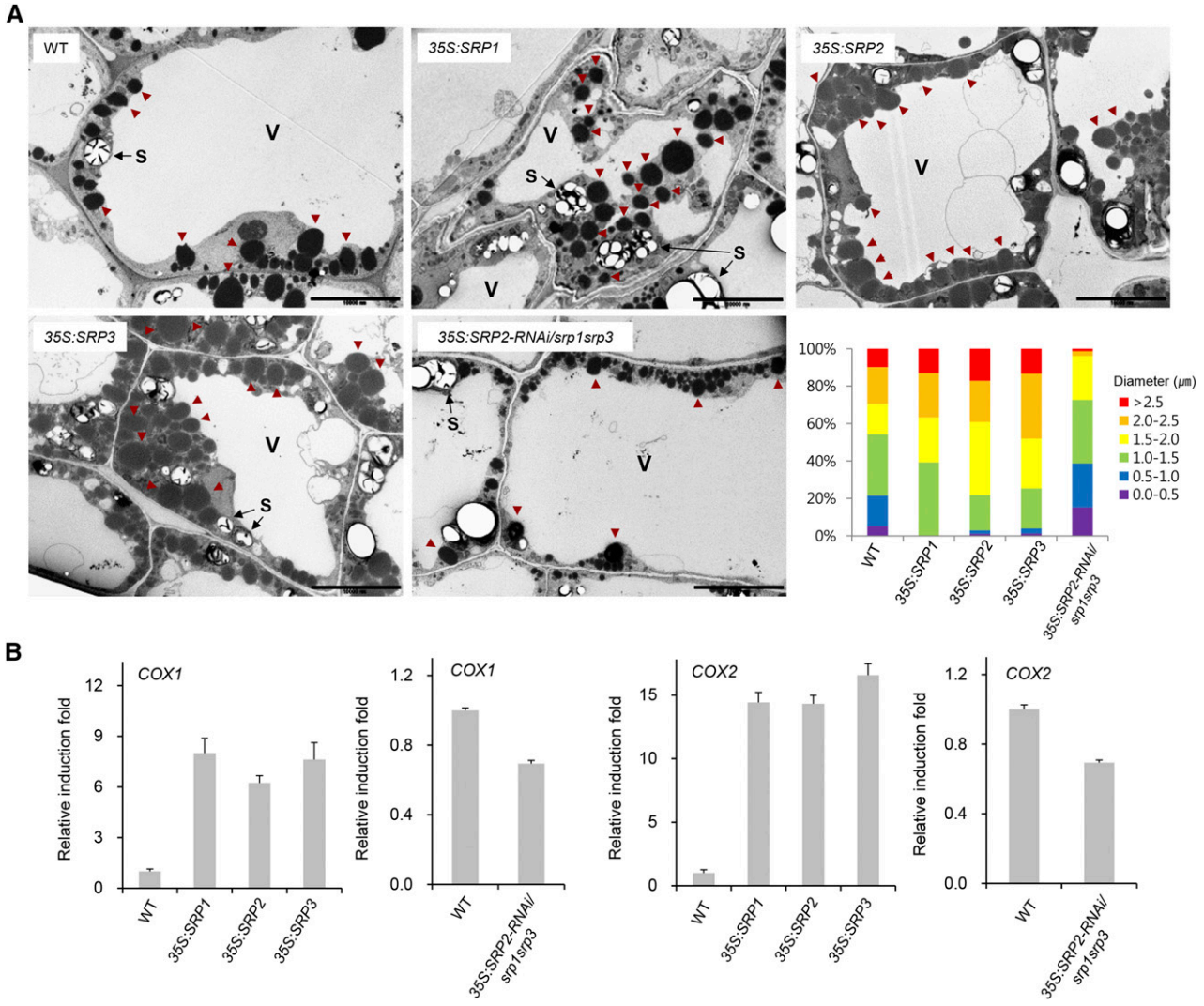

Figure 8. Distribution of LDs and the expression levels of mitochondrial respiratory genes. A, TEM analysis of 6-d-old hypocotyls from wild-type (WT), *SRP* over-expressors, and *35S:SRP2-RNAi/srp1srp3* triple mutant plants. LDs were divided into six groups (>2.5, 2.0-2.5, 1.5-2.0, 1.0-1.5, 0.5-1.0, and 0.0-0.5 μm) depending on their sizes. Red arrowheads indicate LDs. V, central vacuole; S, starch granule. Scale bars = 10 μm. B, Expression of *COX1* and *COX2*, mitochondrial respiratory marker genes, in wild-type, *35S:SRP* transgenic, and *35S:SRP2-RNAi/srp1srp3* mutant plants. Data represent means ± SD from three independent experiments.

expressed recombinant SRPP displayed the self-assembly property (Berthelot et al., 2014a). Thus, we hypothesized that Arabidopsis SRPs play a role in the formation of LDs via their polymerization properties. To test this hypothesis, the *35S: Flag-SRP* constructs were infiltrated into tobacco leaves. Total protein crude extracts were prepared and analyzed by immuno-gel blot assay. When nondenatured crude extract samples were subjected to native protein gel-blot analysis, high-molecular-weight smear bands of Flag-SRP proteins were detected by anti-Flag antibody (Figure 9A, top). This result was different from that of SDS denaturing PAGE gel that displayed two shifted protein bands (Fig. 1C; Fig. 9A, bottom). Similar results were obtained with bacterially expressed 6×His-2×Flag-SRP recombinant proteins. As shown in Figure 9B, purified 6×His-2×Flag-SRPs exhibited high-molecular-weight ladders in a native PAGE gel (Fig. 9B, lane 1, top). In contrast, these smear bands disappeared when the protein samples were denatured (Fig. 9B, lane 1, bottom). The 6×His-2×Flag-SRPs were denatured by heat in the presence of 0.2% SDS and 100 mM β-mercaptoethanol. The denatured 6×His-2×Flag-SRPs were then renatured by removal of the detergents through dialysis at 28°C for 2 h and subjected to immuno-blot analysis on a native or denaturing PAGE gel. The results showed that high-molecular-mass smear bands were apparent in a native PAGE gel (Fig. 9B, lane 2, top) and, in contrast, dimeric bands were detected in denaturing PAGE gel (Fig. 9B, lane 2,

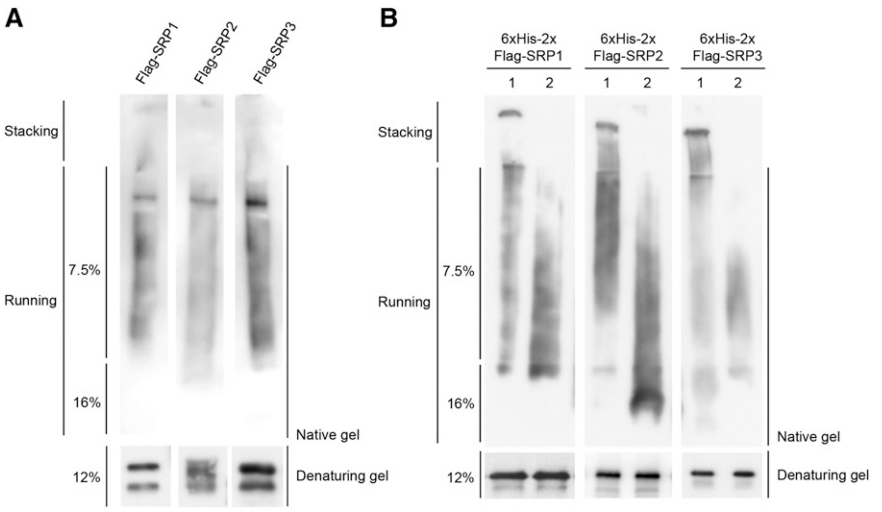

Figure 9. Polymerization properties of SRPs. A, In vivo polymerization of SRPs. Total protein extracts were prepared from *35S:Flag-SRPs*-infiltrated tobacco leaves and subjected to immuno-blot analysis by native (7.5% and 16%; top) or denaturing (12%; bottom) PAGE gel with anti-Flag antibody. B, Lane 1: bacterially expressed 6×His-2×Flag-fused SRPs were purified and subjected to immuno-blot analysis by native (7.5% and 16%; top) or denaturing (12%; bottom) PAGE gel with anti-Flag antibody. Lane 2: 6×His-2×Flag-fused SRPs were boiled in the presence of 0.2% SDS and 100 mM β-mercaptoethanol. Denatured 6×His-2×Flag-SRPs were renatured for 2 h at 28°C and subjected to immuno-blotting by native (top) or denaturing (bottom) PAGE gel with anti-Flag antibody.

bottom). These results suggest that SRPs are polymerized in vivo and in vitro.

DISCUSSION

In this study, we characterized three SRP homologs in Arabidopsis. Similar to rubber tree SRPP, Arabidopsis SRPs appear to be membrane-associated glycoproteins (Fig. 1, C and D). *SRP1*, *SRP2*, and *SRP3* are differentially expressed in various tissues and are induced by a broad spectrum of abiotic stimuli and ABA (Fig. 2). Consistent with their expression profiles, SRPs are positively involved in the growth of both vegetative and reproductive tissues (Figs. 3 and 4), as well as tolerance response to drought stress (Fig. 5). These results suggest that Arabidopsis SRPs play dual roles as positive factors in tissue growth and development and in drought stress response.

Rubber tree SRPP is localized to the surface of rubber particles, which have structural similarities to LDs in non-rubber-producing plants (Schmidt et al., 2010; Berthelot et al., 2014b). In addition, avocado SRP homologs (LDAP1 and LDAP2) and Arabidopsis SRP3 localize to the surface of LDs (Horn et al., 2013). Our current data show that the subcellular localization patterns of SRP1 and SRP2 are very similar to that of SRP3 and are reminiscent of those of LDAP1 and LDAP2 (Fig. 1B). Confocal microscopy with Nile red-stained tobacco leaves strongly indicates that three SRPs are colocalized to LDs (Fig. 7). Thus, SRP1 and SRP2, in addition to SRP3, are likely associated with LDs. SRPP in rubber tree participates in rubber particle aggregation and latex coagulation (Wititsuwannakul et al., 2008). Arabidopsis SRPs are related with the number and size of LDs, as evidenced by the results that over-expression of *SRPs* resulted in the accumulation of large-sized LDs in seedlings (Fig. 8) and that SRPs displayed in vivo and in vitro polymerization properties (Fig. 9). Thus, it seems that the cellular roles of SRP homologs are conserved, at least in part, in rubber-producing and non-rubber-producing plants.

Because LDs store neutral lipids, their biogenesis is closely related to cell proliferation in both mammalian and plant systems (Siloto et al., 2006; Yonezawa et al., 2011). Regulation of adipocytes, which are specialized tissues for lipid storage, is an important concern in human diseases such as diabetes and obesity (Gong et al., 2011). For example, fat-specific protein 27 (Fsp27) is a mammalian LD-associated protein that regulates LD biogenesis and affects cellular respiratory rate in the *ob* mouse (Yonezawa et al., 2011). In higher plants, LDs participate in cell proliferation in the seedling establishment stage by providing neutral lipids as carbon sources, while the cellular roles of LDs in postgermination growth are not well understood (Siloto et al., 2006). Studies on plant LD-associated proteins, including oleosins, caleosins, oil body-associated protein (OBAPs), and SEIPIN, have mainly focused on seed development and germination (López-Ribera et al., 2014; Cai et al., 2015). On the other hand, expression of Arabidopsis *SRPs* has been detected in postgermination tissues, including roots, leaves, and flowers (Fig. 2, A and B), and SRPs participate in postgermination growth and early bolting (Figs. 3 and 4). Furthermore, the germination profiles of *SRP*-over-expressing and mutant lines were undistinguishable from that of the wild-type (Fig. 3A). Thus, SRPs play a role in postgermination Arabidopsis growth. This view is further supported by the results that cell wall marker genes (*WAK1*, *FEI2*, and *PME3*) and mitochondrial respiratory genes (*COX1* and *COX2*) were up-regulated in postgermination seedlings of *SRP*-over-expressing plants (Figs. 6B and 8B). The predicted amino acid sequence alignment revealed that the monocot model crop rice, which produces glutelin-rich seeds, contains two SRP homologs (Supplemental Fig. S1, A and B). Overall, we speculate that the LD-associated SRP homologs are involved in the broad aspects of tissue growth and development in non-rubber-producing plants.

Responsive to Dehydration 20 is a stress-inducible caleosin that is involved in the drought stress response

(Aubert et al., 2010). Caleosin families were thus named because they possess calcium-binding sites comprised of a helix-loop-helix EF-hand motif (Laibach et al., 2015). Because calcium is a critical factor in the stress-signaling pathway, LD-associated caleosins participate in plant stress responses in addition to their structural role in LDs. These results may provide clues to the functions of LDs in stress responses (Purkrtova et al., 2008). Our data (Fig. 5) and previous results obtained by other groups show that LD-associated SRP homologs function as positive factors in abiotic stress responses (Kim et al., 2010; Seo et al., 2010; Balbuena et al., 2011; Fricke et al., 2013; Gidda et al., 2013). LDs serve as a reservoir for isoprenoids and steroid compounds, as well as neutral lipids, which act as hormones and/or antioxidant molecules. Thus, one cannot discount the possibility that LDs mediate stress responses by regulating these lipid compounds. This is consistent with the notion that SRPs confer enhanced drought tolerance by promoting the biogenesis of LDs (Fig. 8A).

An additional property of LDs as a protein-storage depot is that they store extra-nuclear histones and may provide histones to the nuclei for efficient chromatin assembly during times of high demand (Cermelli et al., 2006; Li et al., 2012). Spatiotemporal regulation of histones by LDs may control the expression of a subset of genes during cellular proliferation and in response to stress, which in turn, increases tissue growth and tolerance against stress such as drought. It should be noted that, because different kinds of proteins are associated with LDs, molecular crowding is a key factor in the determination of the composition of LD-associated proteins (Kory et al., 2015). Thus, it is plausible that various LD-associated proteins such as SRPs are involved in different but interconnected cellular aspects, including tissues growth and stress responses. Further experiments are required to identify additional LD-associated proteins and uncover their roles in the regulation LD biogenesis and drought stress tolerance in Arabidopsis.

It is noteworthy that, among the three SRP homologs, the expression level of SRP2 was very low in most tissues examined and was selectively induced by drought (Fig. 2). The *35S:SRP2-RNAi* knock-down plants exhibited wild-type-like phenotypes in terms of tissue growth (Figs. 3 and 4), but they were extremely sensitive to dehydration stress. In addition, a high level of *SRP2* transcript was exceptionally detected in developing seeds (Fig. 2A). SRP2 contains an acidic pI value of 4.4, whereas those of SRP1 and SRP3 are close to neutral (8.9 and 8.3, respectively). More diverse putative cis-acting regulatory elements exist in the upstream region of *SRP2* compared to those of *SRP1* and *SRP3* (Supplemental Table S2). Thus, although SRP1, SRP2, and SRP3 play combinatory roles in diverse cellular aspects, there might be a functional specificity among the three SRPs in Arabidopsis.

Another interesting result is that Arabidopsis SRPs have polymerization properties (Fig. 9). Polymerization patterns of SRPs were indistinguishable in vivo and in vitro and, thus, it seems likely that glycosylation may not be essential for polymerization of these Arabidopsis proteins. Similarly, rubber tree SRPP exhibits latex coagglutination activity and self-assembly activity in vitro (Wititsuwannakul et al., 2008; Berthelot et al., 2014b). Other LD-associated proteins, including FSP27 and SEIPIN, act as oligomers to regulate size of LD (Chapman et al., 2012; Cai et al., 2015). These indicate that homo- or hetero-oligomerization of LD-associated proteins is involved in the biogenesis of LDs.

It should be noted that SRPs were not detected in Arabidopsis LD proteome data from mature leaves and seeds (Jolivet et al., 2004; Shimada et al., 2014). One possibility is that expression of *SRPs* are tightly regulated transcriptionally (Fig. 2) and/or posttranslationally in response to developmental process and environmental stress. SRPs are routinely solubilized from the membrane fraction in the presence of detergent (Fig. 1C). Thus, it is also possible that SRPs are associated with LDs transiently and/or reversibly under certain conditions (e.g. in response to drought stress and in mature leaves). Formation of LDs was induced by unfavorable growth conditions, such as nitrogen starvation, excess lipids, and ER stress, in animals, yeasts, and algae (Hapala et al., 2011; Siaut et al., 2011; Krahmer et al., 2013). Recently, Cai et al. (2015) reported that LD-associated protein SEIPIN promotes LD biogenesis in Arabidopsis. These results are consistent with our data that transgenic Arabidopsis seedlings, in which stress-induced *SRPs* are constitutively expressed, display markedly increased number of LDs as compared to wild-type seedlings (Fig. 8A). Thus, it would be intriguing to examine whether LDs may play as an intermediary host to shuttle SRPs to other organelles and/or cytosolic fractions in response to abiotic stress and developmental processes.

In conclusion, our data suggest that LD-associated SRPs play dual roles as positive factors in tissue growth and development and in drought stress responses in Arabidopsis. These results are consistent with the view that biogenesis and proper functioning of LDs are critical not only to seed development and germination but also to broad physiological aspects in non-rubber-producing Arabidopsis.

MATERIALS AND METHODS

Plant Materials and Stress Treatments

Arabidopsis (*Arabidopsis thaliana*) ecotype Columbia wild-type and T-DNA-inserted loss-of-function *srp1* (GABI_309G05) and *srp3* (Salk_103065) mutant seeds were obtained from the Ohio State University Arabidopsis Biological Resources Center (Columbus, OH). Homozygous *srp1* and *srp3* mutant lines were isolated by genotyping PCR using T-DNA left border and gene-specific primers (Supplemental Table S1). Full-length *SRP1* (Arabidopsis Biological Resources Center stock no. U11034), *SRP2* (U24879), and *SRP3* (U137621) cDNAs were cloned into the binary vector pBI121. *SRP*-over-expressing transgenic lines were generated as described previously (Seo et al., 2008). The RNAi-mediated knock-down construct of *SRP2* (*35S:SRP2-RNAi*) was introduced into the wild-type and *srp1srp3* double mutant plants. The expression levels of *SRPs* in transgenic and mutant progeny were investigated by RT-PCR using gene-specific primer sets (Supplemental Table S1). Wild-type, mutant

(*srp1*, *35S:SRP2-RNAi*, *srp3*, and *35S:SRP2-RNAi/srp1srp3*), and *SRP*-over-expressing plants were treated with ABA (100 μM for 0, 1.5, and 3 h), drought (0, 1.5, and 3 h), low temperature (4°C for 0, 1.5, and 3 h), or high salinity (300 mM NaCl for 0 and 4.5 h) as described by Ryu et al. (2010).

Protoplast Transient Assay

Full-length *SRP* cDNAs were fused with a soluble-modified GFP (*smGFP*), and the *35S:SRP-GFP* constructs were transiently expressed in tobacco (*Nicotiana benthamiana*) leaves by the infiltration method (Kim and Kim, 2013). After 3 d of infiltration, protoplasts were prepared as described by Seo et al. (2008). Expression and subcellular localization of SRP-GFP were monitored with a cooled CCD camera and a BX51 fluorescence microscope (Olympus, Tokyo, Japan) as described previously (Son et al., 2009).

Protein Assays

The *35S:Flag-SRP* fusion genes were constructed using gene-specific primers (Supplemental Table S1) and were transiently coexpressed with *35S:P19* in tobacco leaves via *Agrobacterium*-mediated infiltration. P19, a viral suppressor of posttranscriptional gene-silencing, was used to increase infiltration efficiency (Hellens et al., 2005). For the membrane-association assay, total proteins were extracted from tobacco leaves using a protein-extraction buffer (150 mM NaCl, 1 mM EDTA, and 50 mM Tris-HCl buffer, pH 7.4) with or without 1% Triton X-100 (Phan et al., 2008). After 15 min of incubation, samples were centrifuged at 16,000 *g* for 10 min at 4°C. The supernatant and pellet fractions were analyzed by immuno-blotting with anti-Flag antibody.

For the lectin-binding assay, total proteins were prepared with the protein-extraction buffer containing 1% Triton X-100 and incubated with Con A-sepharose resin at 4°C overnight in the presence or absence of methyl α-D-glucopyranoside. Flag-fused KOR1-Flag was used as a positive marker for glycoproteins. After incubation, the sepharose resin was washed with the protein-extraction buffer, and bound proteins were eluted by boiling in SDS sample buffer. The eluted proteins were subjected to protein gel-blot analysis using the anti-Flag antibody (Park et al., 2010).

RNA Extraction, cDNA Synthesis, and qRT-PCR

Total RNA was isolated from developing tissues, including seedlings, roots, leaves, stems, flowers, siliques, and seeds, and from abiotic stress- or ABA-treated 7-d-old seedlings using the RNAiso RNA purification kit according to the manufacturer's protocol (Takara, Shiga, Japan) with slight modifications as described by Xu et al. (2014). Total RNA was treated with DNase I (Promega, Madison, WI) for 30 min, and then, first-strand cDNA was synthesized as described by Kim et al. (2010). RT-PCR was performed using gene-specific primer sets (Supplemental Table S1). qRT-PCR was performed using an IQ5 light cycler (Bio-Rad, Hercules, CA), and the results were analyzed using the IQ5 optical system software (Bio-Rad), as described by Kim and Kim (2013).

Histochemical GUS Assay

The promoter regions of three *SRPs* were analyzed using the AGRIS program (Arabidopsis Gene Regulatory Information Server, http://arabidopsis.med.ohio-state.edu/AticsDB; promoter ID: *SRP1*, At1g67360; *SRP2*, At2g47780; and *SRP3*, At3g05500). The *promoter-SRP-GUS* constructs (*pSRP1-GUS*, *pSRP2-GUS*, and *pSRP3-GUS*) were introduced into Arabidopsis as described previously (Cho et al., 2011). For GUS staining, T3 *pSRP-GUS* transgenic plants were immersed in 50 mM sodium phosphate buffer (pH 7.2) containing 2 mM cyclohexylammonium salt (Duchefa Biochemie, Haarlem, Netherlands), 0.5 mM $K_3Fe(CN)_6$, and 0.5 mM $K_4Fe(CN)_6$, and incubated overnight at 37°C as described previously (Yoon et al., 2014). Chlorophyll was removed from the GUS-stained tissue by treatment with 70% ethanol for 6 h.

Phenotypic Analyses

For the germination assay, wild-type, *SRP*-overexpressing transgenic, and *srp* loss-of-function mutant seeds were collected at the same time and grown on half-strength Murashige and Skoog medium supplemented with vitamins and 1% Suc at 22°C with continuous light. The percentages of radicle emergence were calculated 1 to 5 d after sowing. Growth of root and leaf tissues was monitored with the image-analyzing program SCIONIMAGE (Scion Corp., Frederic, MD) as described by Seo et al. (2008). For the microscopic analysis, 3-d-old roots were stained with propidium iodide and visualized using confocal microscopy (LSM510 META; Carl Zeiss, Oberkochen, Germany) as described by Seo et al. (2008). For leaf cell layer observation, 5-d-old leaves were cleared with chloral-hydrate solution, and the images were analyzed using light-field microscopy (BX51 fluorescence microscope, Olympus).

Drought Stress Analysis

Light-grown, 2- to 3-week-old wild-type, *35S:SRP* transgenic, and *srp* mutant plants were subjected to drought stress by withholding water for 8 to 10 d. The plants were then rewatered, and their survival rates were determined after 3 d of rewatering (Kim et al., 2010). Total chlorophyll (chlorophyll a + chlorophyll b) was extracted from the drought-treated leaves as described previously by Bae et al. (2009). The amount of Pro in normal and drought-treated leaves was determined as described by Claussen (2005).

SEM and TEM

The surface structures of wild-type, *SRP*-over-expressing, and *srp*-mutant seeds were examined by high-resolution SEM (model S-800, FESEM, Hitachi, Tokyo, Japan) at an accelerating voltage of 3 kV under high vacuum conditions (Penfield et al., 2001; Atia et al., 2009). For TEM, hypocotyl tissues of 6-d-old seedlings were fixed in 2.5% (v/v) glutaraldehyde, 4% (v/v) formaldehyde, and 100 mM phosphate buffer, pH 7.2, as described by Kim et al. (2011). Thin sections of tissues were prepared using an ultra-microtome (Leica, Vienna, Austria).

Colocalization assays of Arabidopsis SRPs to LDs

The *35S:P19*, *35S:P19 + 35S:LEC2*, and *35S:P19 + 35S:LEC2 + 35S:SRPs-GFP* constructs were transiently expressed in tobacco leaves. P19 was used to increase infiltration efficiency (Hellens et al., 2005). LEC2 is a transcription regulator and was used to promote lipid accumulation and increase number of LDs (Cai et al., 2015). After 3 d of infiltration, tobacco leaves were stained with 2 μg/mL Nile red (Sigma-Aldrich, St. Louis, MO) in 50 mM PIPES buffer (pH 7.0). LDs were imaged using a LSM700 confocal laser scanning microscope (Carl Zeiss). To detect fluorescent signals of GFP and Nile red, samples were excited by 488-nm laser and the emission was acquired from 500 to 540 nm and 560 to 620 nm, respectively.

SRP Polymerization Assay

The 2×Flag-tagged *SRP* constructs were ligated into the pProEX vector (Invitrogen, Carlsbad, CA) and introduced into BL21 (DE3) *E. coli* strain. Expression of *6×His-2×Flag-SRPs* was induced by the addition of IPTG (0.3 mM) into the growth medium and expressed recombinant proteins were purified using the Ni-NTA system according to the manufacturer's protocol (QIAGEN, Hilden, Germany). The *35S:Flag-SRP* constructs were infiltrated into tobacco leaves. The bacterially purified 6×His-2×Flag-SRPs and total crude protein extracts of *Flag-SRPs*-expressing leaves were boiled for 10 min in TBS containing 0.2% SDS and 100 mM β-mercaptoethanol for protein denaturation. The denatured SRPs were then renatured by removal of detergent through dialysis at 28°C for 2 h and subjected to native (7.5% and 16%) or denaturing (12%) PAGE followed by immuno-blot analysis using anti-Flag antibody.

Accession Numbers

Sequence data from this article can be found in the GenBank/EMBL data libraries under accession numbers *SRP1* (NP_176904), *SRP2* (NP_182299), and *SRP3* (NP_187201).

Supplemental Data

The following supplemental materials are available.

Supplemental Figure S1. Sequence analysis of Arabidopsis SRPs.

Supplemental Figure S2. Expression profiles of *SRPs*.

Supplemental Figure S3. Generation and isolation of *SRP*-overexpressing and T-DNA-inserted *srp* mutant plants.

Supplemental Figure S4. Number of columella cells in seed coats of wild-type, *SRPs*-over-expressing, and mutant plants.

Supplemental Table S1. The sequence of primers used in this study.

Supplemental Table S2. Sequence analysis of upstream regions of three SRP genes.

Received January 30, 2016; accepted February 18, 2016; published February 22, 2016.

LITERATURE CITED

Abe H, Yamaguchi-Shinozaki K, Urao T, Iwasaki T, Hosokawa D, Shinozaki K (1997) Role of Arabidopsis MYC and MYB homologs in drought- and abscisic acid-regulated gene expression. Plant Cell **9:** 1859–1868

Aon MA, Bhatt N, Cortassa SC (2014) Mitochondrial and cellular mechanisms for managing lipid excess. Front Physiol **5:** 282

Atia A, Debez A, Barhoumi Z, Abdelly C, Smaoui A (2009) Histochemical localization of essential oils and bioactive substances in the seed coat of the halophyte *Crithmum maritimum* L. (Apiaceae). J Plant Biol **52:** 448–452

Aubert Y, Vile D, Pervent M, Aldon D, Ranty B, Simonneau T, Vavasseur A, Galaud JP (2010) RD20, a stress-inducible caleosin, participates in stomatal control, transpiration and drought tolerance in *Arabidopsis thaliana*. Plant Cell Physiol **51:** 1975–1987

Bae H, Choi SM, Yang SW, Pai H-S, Kim WT (2009) Suppression of the ER-localized AAA ATPase NgCDC48 inhibits tobacco growth and development. Mol Cells **28:** 57–65

Balbuena TS, Salas JJ, Martínez-Force E, Garcés R, Thelen JJ (2011) Proteome analysis of cold acclimation in sunflower. J Proteome Res **10:** 2330–2346

Bartz R, Li WH, Venables B, Zehmer JK, Roth MR, Welti R, Anderson RGW, Liu P, Chapman KD (2007) Lipidomics reveals that adiposomes store ether lipids and mediate phospholipid traffic. J Lipid Res **48:** 837–847

Berthelot K, Lecomte S, Estevez Y, Coulary-Salin B, Peruch F (2014a) Homologous *Hevea brasiliensis* REF (Hevb1) and SRPP (Hevb3) present different auto-assembling. Biochim Biophys Acta **1844:** 473–485

Berthelot K, Lecomte S, Estevez Y, Peruch F (2014b) *Hevea brasiliensis* REF (Hev b 1) and SRPP (Hev b 3): An overview on rubber particle proteins. Biochimie **106:** 1–9

Bohnert HJ, Gong Q, Li P, Ma S (2006) Unraveling abiotic stress tolerance mechanisms–getting genomics going. Curr Opin Plant Biol **9:** 180–188

Bray EA (1997) Plant responses to water deficit. Trends Plant Sci **2:** 48–54

Cai Y, Goodman JM, Pyc M, Mullen RT, Dyer JM, Chapman KD (2015) Arabidopsis SEIPIN Proteins Modulate Triacylglycerol Accumulation and Influence Lipid Droplet Proliferation. Plant Cell **27:** 2616–2636

Carman GM (2012) Thematic minireview series on the lipid droplet, a dynamic organelle of biomedical and commercial importance. J Biol Chem **287:** 2272

Cermelli S, Guo Y, Gross SP, Welte MA (2006) The lipid-droplet proteome reveals that droplets are a protein-storage depot. Curr Biol **16:** 1783–1795

Chapman KD, Dyer JM, Mullen RT (2012) Biogenesis and functions of lipid droplets in plants: thematic review series: lipid droplet synthesis and metabolism: from yeast to man. J Lipid Res **53:** 215–226

Chapman KD, Dyer JM, Mullen RT (2013) Commentary: why don't plant leaves get fat? Plant Sci **207:** 128–134

Chapman KD, Ohlrogge JB (2012) Compartmentation of triacylglycerol accumulation in plants. J Biol Chem **287:** 2288–2294

Cho SK, Ryu MY, Seo DH, Kang BG, Kim WT (2011) The Arabidopsis RING E3 ubiquitin ligase AtAIRP2 plays combinatory roles with AtAIRP1 in abscisic acid-mediated drought stress responses. Plant Physiol **157:** 2240–2257

Choi H, Hong J, Ha J, Kang J, Kim SY (2000) ABFs, a family of ABA-responsive element binding factors. J Biol Chem **275:** 1723–1730

Claussen W (2005) Proline as a measure of stress in tomato plants. Plant Sci **168:** 241–248

Cornish K, Wood DF, Windle JJ (1999) Rubber particles from four different species, examined by transmission electron microscopy and electron-paramagnetic-resonance spin labeling, are found to consist of a homogeneous rubber core enclosed by a contiguous, monolayer biomembrane. Planta **210:** 85–96

de Vetten NC, Ferl RJ (1995) Characterization of a maize G-box binding-factor that is induced by hypoxia. Plant J **7:** 589–601

Eastmond PJ (2006) SUGAR-DEPENDENT1 encodes a patatin domain triacylglycerol lipase that initiates storage oil breakdown in germinating Arabidopsis seeds. Plant Cell **18:** 665–675

Farese RV Jr, Walther TC (2009) Lipid droplets finally get a little R-E-S-P-E-C-T. Cell **139:** 855–860

Fontanesi F, Soto IC, Barrientos A (2008) Cytochrome c oxidase biogenesis: new levels of regulation. IUBMB Life **60:** 557–568

Fricke J, Hillebrand A, Twyman RM, Prüfer D, Schulze Gronover C (2013) Abscisic acid-dependent regulation of small rubber particle protein gene expression in *Taraxacum brevicorniculatum* is mediated by TbbZIP1. Plant Cell Physiol **54:** 448–464

Gidda SK, Watt S, Collins-Silva J, Kilaru A, Arondel V, Yurchenko O, Horn PJ, James CN, Shintani D, Ohlrogge JB, Chapman KD, Mullen RT, et al (2013) Lipid droplet-associated proteins (LDAPs) are involved in the compartmentalization of lipophilic compounds in plant cells. Plant Signal Behav **8:** e27141

Gong J, Sun Z, Wu L, Xu W, Schieber N, Xu D, Shui G, Yang H, Parton RG, Li P (2011) Fsp27 promotes lipid droplet growth by lipid exchange and transfer at lipid droplet contact sites. J Cell Biol **195:** 953–963

Guo Y, Cordes KR, Farese RV Jr, Walther TC (2009) Lipid droplets at a glance. J Cell Sci **122:** 749–752

Hapala I, Marza E, Ferreira T (2011) Is fat so bad? Modulation of endoplasmic reticulum stress by lipid droplet formation. Biol Cell **103:** 271–285

Hellens RP, Allan AC, Friel EN, Bolitho K, Grafton K, Templeton MD, Karunairetnam S, Gleave AP, Laing WA (2005) Transient expression vectors for functional genomics, quantification of promoter activity and RNA silencing in plants. Plant Methods **1:** 13

Herker E, Ott M (2012) Emerging role of lipid droplets in host/pathogen interactions. J Biol Chem **287:** 2280–2287

Hong JP, Kim WT (2005) Isolation and functional characterization of the *Ca-DREBLP1* gene encoding a dehydration-responsive element binding-factor-like protein 1 in hot pepper (*Capsicum annuum* L. cv. Pukang). Planta **220:** 875–888

Horn PJ, James CN, Gidda SK, Kilaru A, Dyer JM, Mullen RT, Ohlrogge JB, Chapman KD (2013) Identification of a new class of lipid droplet-associated proteins in plants. Plant Physiol **162:** 1926–1936

Ishitani M, Xiong L, Stevenson B, Zhu JK (1997) Genetic analysis of osmotic and cold stress signal transduction in Arabidopsis: interactions and convergence of abscisic acid-dependent and abscisic acid-independent pathways. Plant Cell **9:** 1935–1949

Jacquier N, Mishra S, Choudhary V, Schneiter R (2013) Expression of oleosin and perilipins in yeast promotes formation of lipid droplets from the endoplasmic reticulum. J Cell Sci **126:** 5198–5209

Jolivet P, Roux E, D'Andrea S, Davanture M, Negroni L, Zivy M, Chardot T (2004) Protein composition of oil bodies in Arabidopsis thaliana ecotype WS. Plant Physiol Biochem **42:** 501–509

Kagaya Y, Ohmiya K, Hattori T (1999) RAV1, a novel DNA-binding protein, binds to bipartite recognition sequence through two distinct DNA-binding domains uniquely found in higher plants. Nucleic Acids Res **27:** 470–478

Khalimonchuk O, Rödel G (2005) Biogenesis of cytochrome c oxidase. Mitochondrion **5:** 363–388

Kim EY, Seo YS, Kim WT (2011) AtDSEL, an Arabidopsis cytosolic DAD1-like acylhydrolase, is involved in negative regulation of storage oil mobilization during seedling establishment. J Plant Physiol **168:** 1705–1709

Kim EY, Seo YS, Lee H, Kim WT (2010) Constitutive expression of *CaSRP1*, a hot pepper small rubber particle protein homolog, resulted in fast growth and improved drought tolerance in transgenic Arabidopsis plants. Planta **232:** 71–83

Kim JH, Kim WT (2013) The Arabidopsis RING E3 ubiquitin ligase AtAIRP3/LOG2 participates in positive regulation of high-salt and drought stress responses. Plant Physiol **162:** 1733–1749

Kim SY, Chung HJ, Thomas TL (1997) Isolation of a novel class of bZIP transcription factors that interact with ABA-responsive and

embryo-specification elements in the Dc3 promoter using a modified yeast one-hybrid system. Plant J **11:** 1237–1251

Kory N, Thiam AR, Farese RV Jr, Walther TC (2015) Protein crowding is a determinant of lipid droplet protein composition. Dev Cell **34:** 351–363

Krahmer N, Farese RV Jr, Walther TC (2013) Balancing the fat: lipid droplets and human disease. EMBO Mol Med **5:** 905–915

Laibach N, Post J, Twyman RM, Gronover CS, Prüfer D (2015) The characteristics and potential applications of structural lipid droplet proteins in plants. J Biotechnol **201:** 15–27

Lamb RS, Hill TA, Tan QKG, Irish VF (2002) Regulation of APETALA3 floral homeotic gene expression by meristem identity genes. Development **129:** 2079–2086

Li Z, Thiel K, Thul PJ, Beller M, Kühnlein RP, Welte MA (2012) Lipid droplets control the maternal histone supply of Drosophila embryos. Curr Biol **22:** 2104–2113

López-Ribera I, La Paz JL, Repiso C, García N, Miquel M, Hernández ML, Martínez-Rivas JM, Vicient CM (2014) The evolutionary conserved oil body associated protein OBAP1 participates in the regulation of oil body size. Plant Physiol **164:** 1237–1249

Micheli F (2001) Pectin methylesterases: cell wall enzymes with important roles in plant physiology. Trends Plant Sci **6:** 414–419

Murphy DJ (2012) The dynamic roles of intracellular lipid droplets: from archaea to mammals. Protoplasma **249:** 541–585

Park SY, Kim HS, Kim NH, Ji S, Cha SY, Kang JG, Ota I, Shimada K, Konishi N, Nam HW, et al (2010) Snail1 is stabilized by O-GlcNAc modification in hyperglycaemic condition. EMBO J **29:** 3787–3796

Penfield S, Meissner RC, Shoue DA, Carpita NC, Bevan MW (2001) MYB61 is required for mucilage deposition and extrusion in the Arabidopsis seed coat. Plant Cell **13:** 2777–2791

Phan NQ, Kim SJ, Bassham DC (2008) Overexpression of Arabidopsis sorting nexin AtSNX2b inhibits endocytic trafficking to the vacuole. Mol Plant **1:** 961–976

Pla M, Vilardell J, Guiltinan MJ, Marcotte WR, Niogret MF, Quatrano RS, Pagès M (1993) The cis-regulatory element CCACGTGG is involved in ABA and water-stress responses of the maize gene rab28. Plant Mol Biol **21:** 259–266

Purkrtova Z, Le Bon C, Kralova B, Ropers MH, Anton M, Chardot T (2008) Caleosin of *Arabidopsis thaliana*: effect of calcium on functional and structural properties. J Agric Food Chem **56:** 11217–11224

Ryu MY, Cho SK, Kim WT (2010) The Arabidopsis C3H2C3-Type RING E3 ubiquitin ligase AtAIRP1 is a positive regulator of an abscisic acid-dependent response to drought stress. Plant Physiol **154:** 1983–1997

Sablowski RWM, Moyano E, Culianez-Macia FA, Schuch W, Martin C, Bevan M (1994) A flower-specific Myb protein activates transcription of phenylpropanoid biosynthetic genes. EMBO J **13:** 128–137

Shimada TL, Takano Y, Shimada T, Fujiwara M, Fukao Y, Mori M, Okazaki Y, Saito K, Sasaki R, Aoki K, et al (2014) Leaf oil body functions as a subcellular factory for the production of a phytoalexin in Arabidopsis. Plant Physiol **164:** 105–118

Schmidt T, Lenders M, Hillebrand A, van Deenen N, Munt O, Reichelt R, Eisenreich W, Fischer R, Prüfer D, Gronover CS (2010) Characterization of rubber particles and rubber chain elongation in *Taraxacum koksaghyz*. BMC Biochem **11:** 11

Seo SG, Kim JS, Yang YS, Jun BK, Kang SW, Lee GP, Kim W, Kim JB, Lee HU, Kim SH (2010) Cloning and characterization of the new multiple stress responsible gene I (*MuSI*) from sweet potato. Genes Genomics **32:** 544–552

Seo YS, Kim EY, Mang HG, Kim WT (2008) Heterologous expression, and biochemical and cellular characterization of *CaPLA1* encoding a hot pepper phospholipase A1 homolog. Plant J **53:** 895–908

Shinozaki K, Yamaguchi-Shinozaki K (1996) Molecular responses to drought and cold stress. Curr Opin Biotechnol **7:** 161–167

Shinozaki K, Yamaguchi-Shinozaki K (2007) Gene networks involved in drought stress response and tolerance. J Exp Bot **58:** 221–227

Siaut M, Cuiné S, Cagnon C, Fessler B, Nguyen M, Carrier P, Beyly A, Beisson F, Triantaphylidès C, Li-Beisson Y, Peltier G (2011) Oil accumulation in the model green alga Chlamydomonas reinhardtii: characterization, variability between common laboratory strains and relationship with starch reserves. BMC Biotechnol **11:** 7

Siloto RMP, Findlay K, Lopez-Villalobos A, Yeung EC, Nykiforuk CL, Moloney MM (2006) The accumulation of oleosins determines the size of seed oilbodies in Arabidopsis. Plant Cell **18:** 1961–1974

Son O, Cho SK, Kim EY, Kim WT (2009) Characterization of three Arabidopsis homologs of human RING membrane anchor E3 ubiquitin ligase. Plant Cell Rep **28:** 561–569

Steinwand BJ, Kieber JJ (2010) The role of receptor-like kinases in regulating cell wall function. Plant Physiol **153:** 479–484

Stork J, Harris D, Griffiths J, Williams B, Beisson F, Li-Beisson Y, Mendu V, Haughn G, Debolt S (2010) CELLULOSE SYNTHASE9 serves a nonredundant role in secondary cell wall synthesis in Arabidopsis epidermal testa cells. Plant Physiol **153:** 580–589

Sun Z, Gong J, Wu H, Xu W, Wu L, Xu D, Gao J, Wu JW, Yang H, Yang M, Li P (2013) Perilipin1 promotes unilocular lipid droplet formation through the activation of Fsp27 in adipocytes. Nat Commun **4:** 1594

Szymanski J, Brotman Y, Willmitzer L, Cuadros-Inostroza Á (2014) Linking gene expression and membrane lipid composition of Arabidopsis. Plant Cell **26:** 915–928

Ulmasov T, Hagen G, Guilfoyle TJ (1999) Dimerization and DNA binding of auxin response factors. Plant J **19:** 309–319

Vij S, Tyagi AK (2007) Emerging trends in the functional genomics of the abiotic stress response in crop plants. Plant Biotechnol J **5:** 361–380

Wilfling F, Haas JT, Walther TC, Farese RV Jr (2014) Lipid droplet biogenesis. Curr Opin Cell Biol **29:** 39–45

Wititsuwannakul R, Rukseree K, Kanokwiroon K, Wititsuwannakul D (2008) A rubber particle protein specific for *Hevea latex* lectin binding involved in latex coagulation. Phytochemistry **69:** 1111–1118

Xu N, Zhang SO, Cole RA, McKinney SA, Guo F, Haas JT, Bobba S, Farese RV Jr, Mak HY (2012) The FATP1-DGAT2 complex facilitates lipid droplet expansion at the ER-lipid droplet interface. J Cell Biol **198:** 895–911

Xu SL, Rahman A, Baskin TI, Kieber JJ (2008) Two leucine-rich repeat receptor kinases mediate signaling, linking cell wall biosynthesis and ACC synthase in Arabidopsis. Plant Cell **20:** 3065–3079

Xu T, Sy ND, Lee HJ, Kwak KJ, Gu L, Kim J-I, Kang H (2014) Functional characterization of a chloroplast-targeted RNA-binding protein CRP1 in *Arabidopsis thaliana* under abiotic stress conditions. J Plant Biol **57:** 349–356

Yang H, Galea A, Sytnyk V, Crossley M (2012) Controlling the size of lipid droplets: lipid and protein factors. Curr Opin Cell Biol **24:** 509–516

Yonezawa T, Kurata R, Kimura M, Inoko H (2011) Which CIDE are you on? Apoptosis and energy metabolism. Mol Biosyst **7:** 91–100

Yoon EK, Kim J-W, Yang JH, Kim S-H, Lim J, Lee WS (2014) A molecular framework for the differential responses of primary and lateral roots to auxin in *Arabidopsis thaliana*. J Plant Biol **57:** 274–281

Zehmer JK, Huang Y, Peng G, Pu J, Anderson RGW, Liu P (2009) A role for lipid droplets in inter-membrane lipid traffic. Proteomics **9:** 914–921

Zhu JK (2002) Salt and drought stress signal transduction in plants. Annu Rev Plant Biol **53:** 247–273